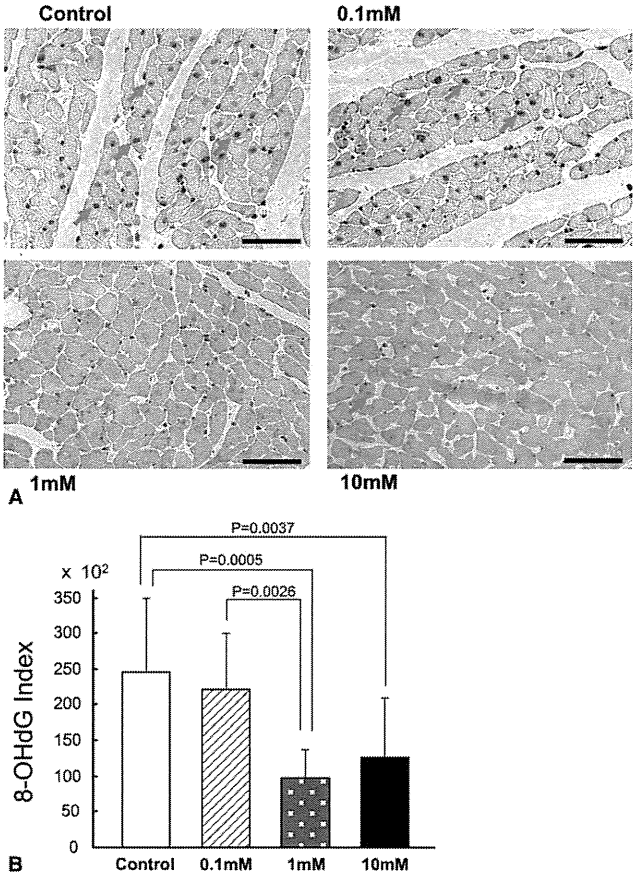

FIGURE 2. Oxidative stress on DNA in cardiomyocytes. A, Representative immunohistochemical analysis images for 8-hydroxy-2′-deoxyguanosine *(8-OHdG)* were obtained with specific monoclonal antibody. Stained nuclei are indicated by *arrows*. *Bar* represents 50 μm. B, Quantification of oxidative stress on DNA, as indicated by 8-hydroxy-2′-deoxyguanosine index. All values shown as mean ± SD.

substrate in caspases known to play an important role in regulating apoptosis, to be blocked by EGCG. In particular, EGCG has been shown to reduce the levels of p38 MAPK phosphorylation,[20] and several studies have confirmed inhibition of p38 MAPK phosphorylation to decrease apoptosis and improve cardiac function after myocardial IRI.[21] Consistent with these findings, our Western blotting analysis demonstrated EGCG to protect against myocardial apoptosis by blocking p38 MAPK phosphorylation and caspase-3 cleavage, indicating that oral pretreatment with EGCG preserved LV function possibly by inhibiting myocardial apoptosis.

Dose Effects of EGCG

In this study, oral pretreatment with a high dose of EGCG did not yield the most potent cardioprotective effects. The cardiac function recovery rates after reperfusion were actually lower in the 10-mmol/L group than in the 1-mmol/L group, despite the blood EGCG concentration remaining higher in the 10-mmol/L group. The plasma EGCG levels of rats given 1-mmol/L EGCG for 2 weeks may have exceeded the saturation point for cardioprotective effects. This result may also, however, be related to some additional adverse effects of EGCG. One possible adverse effect is that EGCG at high concentrations produces an excess of nitric oxide through activation of endothelial nitric oxide synthase. If nitric oxide exceeds a certain level, it reacts with superoxide anion under postischemic reperfusion conditions and yields more toxic radicals, such as hydroxyl radical and peroxynitrite anion, as demonstrated in several studies.[22] The toxic activity of these reaction products may exceed the scavenger activity of EGCG, possibly leading to the suppression of heart function. These results underscore the importance of establishing the optimal oral EGCG dose to maintain recovery of cardiac function and minimize surgical complications, in anticipation of clinical application of EGCG.

Optimal Delivery of EGCG

We advocate that EGCG should be administered orally as a preoperative measure. Recently, with respect to the safety of EGCG, excessively high concentrations have been shown to be cytotoxic and to trigger genotoxic events in mammalian cells.[23] Direct administration of EGCG to the myocardium, such as by intravenous or intracoronary injection, reportedly produces harmful side effects, particularly at high doses. Oral EGCG, however, even when given as a very high bolus dose, is safe in human beings, as shown by clinical trial.[24] In this study, we selected the 2-week oral protocol for administration of EGCG on the basis of a report on the bioavailability of green tea polyphenols in rodents during long-term green tea consumption in drinking fluid.[25] Plasma concentrations of EGCG were shown to gradually increase in the first 2 weeks and then reach a plateau in rats given EGCG in drinking fluid.[25] In considering clinical applications, we will need to establish a period of oral administration of EGCG before heart surgery, referring to several clinical studies to determine the safety and pharmacokinetics of green tea polyphenols with long-term oral administration of EGCG.[24]

Study Limitations

This study has several limitations. First, the heart model used in our experiment may not fully reflect in vivo conditions because of the lack of blood components such as neutrophils, platelets, and blood-derived cytokines. Several studies have demonstrated that neutrophils play an important role in the pathogenesis of IRI. An in vivo study taking into account the influence of blood is therefore in progress. Second, the type of ischemia used in this experimental model was global no-flow ischemia without cardioplegia, which is unlike the type of ischemia used in human heart surgery. This type of ischemia was adopted for this model to facilitate

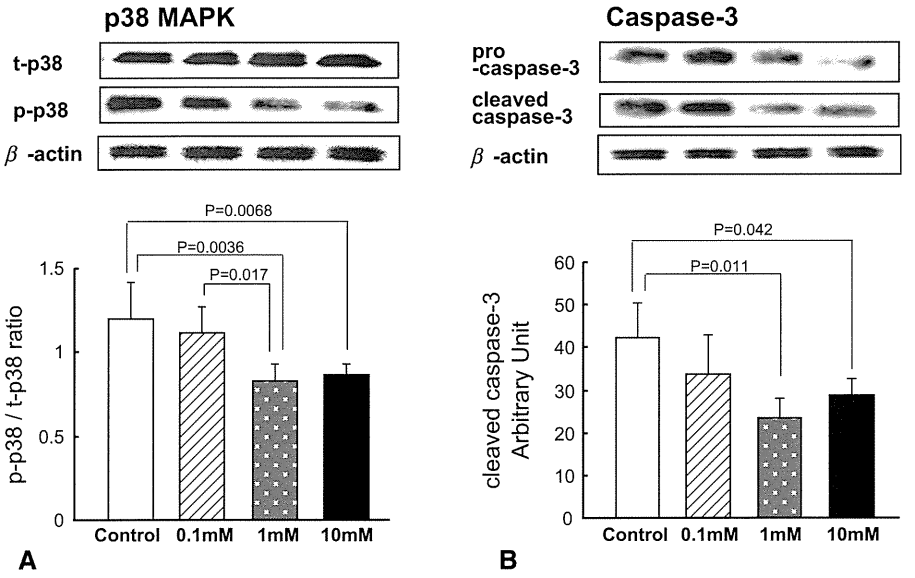

FIGURE 3. Western blotting analysis for apoptosis-related proteins. A, p38 mitogen-activated protein kinase *(MAPK)*, as phosphorylated p38 *(p-p38)* and nonphosphorylated p38 *(t-p38)*. B, Caspase-3. All values shown as mean ± SD.

the evaluation of the cardioprotective effect of EGCG alone, eliminating other cardioprotective factors as far as possible. In the future, further investigations are needed to clarify the cardioprotective effects of oral pretreatment with EGCG in a larger animal model of ischemia with cardioplegia and cardiopulmonary bypass, in view of its clinical application to human heart surgery. These issues will be addressed in future green tea polyphenol clinical trials. Third, in this study, we did not incorporate preischemic measurement of oxidative stress or apoptosis. Although the baseline cardiac function did not differ among the groups, we cannot rule out the possibility that preischemic oxidative stress and apoptosis were suppressed in the EGCG groups. This point needs further investigation. Fourth, the involvement of p38 MAPK expression in apoptosis is still controversial. We cannot definitely conclude that the cardioprotective effect of EGCG exhibited in this study is attributable to p38-mediated apoptosis suppression. We selected p38 for evaluation in this study because in several previous reports EGCG was shown to suppress apoptosis through inhibition of p38 activation under conditions of myocardial IRI.[20]

CONCLUSIONS

Oral pretreatment with EGCG, a green tea polyphenol, attenuated myocardial IRI and enhanced cardiac function recovery after ischemia followed by reperfusion in an isolated rat heart model. The mechanisms of oxidative stress suppression and myocardial apoptosis suppression may be involved in the cardioprotective effects of EGCG. In addition, oral intake of a high dose of EGCG did not dramatically improve cardiac function after ischemia–reperfusion. EGCG pretreatment by oral intake could be a novel and simple preconditioning cardioprotective method for preventing perioperative cardiac dysfunction in cardiac surgical patients.

We thank Ms Fumiyo Kataoka for her expert technical assistance and Dr Fumio Nanjo and Mr Shuichi Otani (Mitsui Norin Co, Ltd, Food Res Labs, Fujieda, Japan) for measuring EGCG concentrations in blood.

References

1. Verma S, Fedak PW, Weisel RD, Butany J, Rao V, Maitland A, et al. Fundamentals of reperfusion injury for the clinical cardiologist. *Circulation*. 2002;105:2332-6.
2. Ferrari R, Agnoletti L, Comini L, Gaia G, Bachetti T, Cargnoni A, et al. Oxidative stress during myocardial ischaemia and heart failure. *Eur Heart J*. 1998;19(Suppl B):B2-11.
3. Visioli F, Keaney JF, Halliwell B. Antioxidants and cardiovascular disease; panaceas or tonics for tired sheep? *Cardiovasc Res*. 2000;47:409.
4. Wu TW, Zeng LH, Wu J, Fung KP. Myocardial protection of MCI-186 in rabbit ischemia–reperfusion. *Life Sci*. 2002;71:2249-55.
5. Wang S, Dusting GJ, May CN, Woodman OL. 3′,4′-Dihydroxyflavonol reduces infarct size and injury associated with myocardial ischaemia and reperfusion in sheep. *Br J Pharmacol*. 2004;142:443-52.
6. Zaveri NT. Green tea and its polyphenolic catechins: medicinal uses in cancer and noncancer applications. *Life Sci*. 2006;78:2073-80.
7. Sano J, Inami S, Seimiya K, Ohba T, Sakai S, Takano T, et al. Effects of green tea intake on the development of coronary artery disease. *Circ J*. 2004;68:665-70.
8. Kuriyama S, Shimazu T, Ohmori K, Kikuchi N, Nakaya N, Nishino Y, et al. Green tea consumption and mortality due to cardiovascular disease, cancer, and all causes in Japan: the Ohsaki study. *JAMA*. 2006;296:1255-65.
9. Higdon JV, Frei B. Tea catechins and polyphenols: health effects, metabolism, and antioxidant functions. *Crit Rev Food Sci Nutr*. 2003;43:89-143.
10. Yamazaki K, Miwa S, Ueda K, Tanaka S, Toyokuni S, Unimonh O, et al. Prevention of myocardial reperfusion injury by poly(ADP-ribose) synthetase inhibitor, 3-aminobenzamide, in cardioplegic solution: in vitro study of isolated rat heart model. *Eur J Cardiothorac Surg*. 2004;26:270-5.
11. Miwa S, Yamazaki K, Hyon SH, Komeda M. A novel method of 'preparative' myocardial protection using green tea polyphenol in oral uptake. *Interact Cardiovasc Thorac Surg*. 2004;3:612-5.
12. Lin LC, Wang MN, Tseng TY, Sung JS, Tsai TH. Pharmacokinetics of (–)-epigallocatechin-3-gallate in conscious and freely moving rats and its brain regional distribution. *J Agric Food Chem*. 2007;55:1517-24.

13. Kasai H, Nishimura S. Hydroxylation of deoxyguanosine at the C-8 position by ascorbic acid and other reducing agents. *Nucleic Acids Res.* 1984;12:2137-45.
14. Toyokuni S. Reactive oxygen species-induced molecular damage and its application in pathology. *Pathol Int.* 1999;49:91-102.
15. Toyokuni S, Tanaka T, Hattori Y, Nishiyama Y, Yoshida A, Uchida K, et al. Quantitative immunohistochemical determination of 8-hydroxy-2′-deoxyguanosine by a monoclonal antibody N45.1: its application to ferric nitrilotriacetate-induced renal carcinogenesis model. *Lab Invest.* 1997;76:365-74.
16. Kanemitsu N, Tambara K, Premaratne GU, Kimura Y, Tomita S, Kawamura T, et al. Insulin-like growth factor-1 enhances the efficacy of myoblast transplantation with its multiple functions in the chronic myocardial infarction rat model. *J Heart Lung Transplant.* 2006;25:1253-62.
17. Gross GJ, Kersten JR, Warltier DC. Mechanisms of postischemic contractile dysfunction. *Ann Thorac Surg.* 1999;68:1898-904.
18. McColl AJ, Keeble T, Hadjinikolaou L, Cohen A, Aitkenhead H, Glenville B, et al. Plasma antioxidants: evidence for a protective role against reactive oxygen species following cardiac surgery. *Ann Clin Biochem.* 1998;35:616-23.
19. Kumar D, Lou H, Singal PK. Oxidative stress and apoptosis in heart dysfunction. *Herz.* 2002;27:662-8.
20. Townsend PA, Scarabelli TM, Pasini E, Gitti G, Menegazzi M, Suzuki H, et al. Epigallocatechin-3-gallate inhibits STAT-1 activation and protects cardiac myocytes from ischemia/reperfusion-induced apoptosis. *FASEB J.* 2004;18:1621-3.
21. Ma XL, Kumar S, Gao F, Louden CS, Lopez BL, Christopher TA, et al. Inhibition of p38 mitogen-activated protein kinase decreases cardiomyocyte apoptosis and improves cardiac function after myocardial ischemia and reperfusion. *Circulation.* 1999;99:1685-91.
22. Nonami Y. The role of nitric oxide in cardiac ischemia–reperfusion injury. *Jpn Circ J.* 1997;61:119-32.
23. Bandele OJ, Osheroff N. (–)-Epigallocatechin gallate, a major constituent of green tea, poisons human type II topoisomerases. *Chem Res Toxicol.* 2008;21:936-43.
24. Chow HH, Cai Y, Hakim IA, Crowell JA, Shahi F, Brooks CA, et al. Pharmacokinetics and safety of green tea polyphenols after multiple-dose administration of epigallocatechin gallate and polyphenon E in healthy individuals. *Clin Cancer Res.* 2003;9:3312-9.
25. Kim S, Lee MJ, Hong J, Li C, Smith TJ, Yang GY, et al. Plasma and tissue levels of tea catechins in rats and mice during chronic consumption of green tea polyphenols. *Nutr Cancer.* 2000;37:41-8.

Acta Biomaterialia 8 (2012) 1792–1801

Contents lists available at SciVerse ScienceDirect

Acta Biomaterialia

journal homepage: www.elsevier.com/locate/actabiomat

Enhanced angiogenesis by multiple release of platelet-rich plasma contents and basic fibroblast growth factor from gelatin hydrogels

Makoto Matsui, Yasuhiko Tabata *

Department of Biomaterials, Field of Tissue Engineering, Institute for Frontier Medical Sciences, Kyoto University, 53 Kawahara-cho Shogoin, Sakyo-ku, Kyoto 606-8507, Japan

ARTICLE INFO

Article history:
Received 20 October 2011
Received in revised form 27 December 2011
Accepted 13 January 2012
Available online 21 January 2012

Keywords:
Gelatin hydrogel
PRP
bFGF
Controlled release
Angiogenesis

ABSTRACT

The objective of this study is to evaluate the angiogenic effects induced by biodegradable gelatin hydrogel granules incorporating mixed platelet-rich plasma (PRP) growth factor mixture (PGFM) and bioactive basic fibroblast growth factor (bFGF). The PRP was prepared by a double-spinning technique for isolating animal bloods, followed by treatment with different concentrations of calcium chloride ($CaCl_2$) solution. The $CaCl_2$ solution treatment activated the platelets of PRP, allowing the release of various growth factors, such as platelet-derived growth factor (PDGF)-BB, vascular endothelial growth factor (VEGF), transforming growth factor (TGF)-β_1, and epithelial growth factor (EGF). In the PRP treated with different $CaCl_2$ solutions, high amounts of representative platelet growth factor, PDGF-BB, VEGF, EGF, and TGF-β_1 were detected in the $CaCl_2$ concentrations of 1, 2, and 4 wt.% compared with higher or lower ones. The PRP treated was impregnated into gelatin hydrogel granules freeze-dried at 37 °C for 1 h, and then the percentage of PGFM desorbed from the gelatin hydrogel granules was evaluated. The percentages of PDGF-BB, VEGF, EGF, and TGF-β_1 desorbed tended to decrease with decreasing $CaCl_2$ concentration. Taken together, the $CaCl_2$ concentration to activate PRP for PGFM release was fixed at 2 wt.%. In vitro release tests demonstrated that the PGFM was released from the gelatin hydrogel granules with time. For the gelatin hydrogels incorporating PGFM and bFGF, the time profile of PDGF-BB or bFGF release was in good correspondence with that of gelatin hydrogel degradation. The gelatin hydrogel granules incorporating mixed PGFM and bFGF were prepared and intramuscularly injected to a mouse leg ischemia model to evaluate the angiogenic effects in terms of histological and laser Doppler perfusion imaging examinations. As controls, hydrogel granules incorporating bFGF, PGFM, and platelet-poor plasma were used for the angiogenic evaluation. The number of blood vessels newly formed and the percentage of anti-α-smooth muscle actin antibody-positive cells increased around ischemic sites injected with the gelatin hydrogel granules incorporating mixed PGFM and bFGF, in marked contrast to other control groups. The blood reperfusion level of ischemic tissues was enhanced by the hydrogel granules incorporating mixed PGFM and bFGF, whereas no enhancement was observed for other groups. It is concluded that the dual-release system of PGFM and bFGF from gelatin hydrogel granules shows promise as a method to enhance angiogenic effects.

1. Introduction

Several treatments for therapeutic angiogenesis have been reported to demonstrate experimental and clinical potential. A number of clinical trials of gene therapy and bone marrow cells transplantation have been carried out. However, the biosafety of genetic materials is not always certain [1–3]. In addition, the invasiveness required to harvest bone marrow cells and the lack of scientific knowledge and related technology for bone marrow cells may be potential risks for cell therapy [4,5]. Another option is to make use of growth factor proteins, which enable cells to naturally induce their biological potential for natural angiogenesis. If the growth factor can be used in vivo with the biological activity remaining, growth-factor-induced angiogenesis is a realistic prospect.

A drug delivery system (DDS) is one plausible technology for enhancing the in vivo biological activity of growth factors. Biodegradable gelatin hydrogels have been designed and prepared for the controlled release of bioactive basic fibroblast growth factor (bFGF) [6], transforming growth factor (TGF)-β_1 [7], platelet-derived growth factor (PDGF)-BB [8], bone morphogenetic protein (BMP)-2 [9–11], and hepatocyte growth factor (HGF) [12,13]. For example, bFGF can be released from gelatin hydrogels, demonstrating the therapeutic potential of angiogenesis in animal models of ischemic legs and hearts or the angiogenesis-induced enhancement of therapeutic efficacy of cell transplantation [14–21]. In addition, a clinical trial has been started to confirm the safety

* Corresponding author. Tel.: +81 75 751 4121; fax: +81 75 751 4646.
E-mail address: yasuhiko@frontier.kyoto-u.ac.jp (Y. Tabata).

1742-7061/$ - see front matter © 2012 Acta Materialia Inc. Published by Elsevier Ltd. All rights reserved.
doi:10.1016/j.actbio.2012.01.016

and feasibility of bFGF release from gelatin hydrogels for patients with clinical limb ischemia of intractable disease [22].

Platelet-rich plasma (PRP) is a source of autologous growth factors, including PDGF, vascular endothelial growth factor (VEGF), TGF-β_1, and epithelial growth factor (EGF). Autologous PRP has been used clinically in a wide variety of surgical treatments for soft and hard tissues [23], such as intractable wounds [24], calvaria [25], or maxillofacial bone defects [26], cosmetic surgery [27,28], spinal problems [29], and neovascularization [30]. Platelet growth factors can also be released from gelatin hydrogels, demonstrating their enhanced activity to induce angiogenesis, or regenerate knee meniscus [31,32], intervertebral discs [33–35], and bone tissues [25,36].

In this study, mixed PRP growth factor mixture (PGFM) and bFGF were incorporated into gelatin hydrogels for multiple releases and the angiogenic effect was evaluated by comparing the release of either PGFM or bFGF from the hydrogels. We have reported that neovascularization can be induced with controlled release of bFGF from gelatin hydrogels. The therapeutic neovascularization generally involves both microvascular and macrovascular processes. At the microvasculatory level, angiogenesis is defined as the sprouting and growth of capillaries, which, however, regress after cessation of bFGF stimulation if pericytes are not recruited properly. Therefore, the stabilization of capillary networks newly created by mural cells (pericytes), known to be recruited by PDGF-BB, is essential for therapeutic neovascularization [37]. The process of capillary maturation needs the recruitment of mural cells mediated by PDGF-BB [37,38]. Taken together, in this study, we attempted multiple controlled release of PGFM and bFGF from the gelatin hydrogel to investigate the maturation of blood vessels newly formed in a murine model of hind limb ischemia. Following the intramuscular injection of gelatin hydrogel granules incorporating mixed PGFM and bFGF into an ischemia model animal, the in vivo angiogenesis was evaluated in terms of histological and laser Doppler perfusion imaging examinations. The $CaCl_2$ treatment condition of PRP to allow the release of platelet growth factors was optimized based on the amount of growth factor released and the release pattern from the hydrogel granules. We examine the time profile of representative platelet growth factors from the hydrogel granules compared with that of hydrogel degradation.

2. Materials and methods

2.1. Preparation of gelatin hydrogel granules

A gelatin sample containing low levels of endotoxin (beMatrix® Gelatin LS-H) with an isoelectric point (IEP) of 5.0, isolated by an alkaline process from the porcine skin, was kindly supplied by Nitta Gelatin Inc. (Osaka, Japan). Biodegradable gelatin hydrogel granules were prepared by the glutaraldehyde (GA, Wako Pure Chemical Industries, Osaka, Japan) cross-linking of an aqueous gelatin solution [6,10,11]. Briefly, after mixing 80 μl of aqueous GA solution (25 wt.%) with 40 g of aqueous gelatin solution (5 wt.%) preheated at 40 °C, the mixed aqueous solution was cast into a polystyrene dish (127.8 × 85.5 mm^2, Thermo Fisher Scientific Inc., MA, USA), which was then left for 12 h at 4 °C to allow the chemical cross-linking of gelatin. The resulting hydrogel sheets were then placed in 100 mM glycine aqueous solution (1 l), followed by agitation at room temperature for 1 h to block the residual aldehyde groups of unreacted GA. The cross-linked hydrogel sheets were twice washed with double-distilled water (DDW). After washing, they were homogenized with a Polytron PT-13000DM system (Central Scientific Commerce Inc., Tokyo, Japan) and separated by sieves to obtain gelatin hydrogel granules with diameters ranging from 32 to 52 μm in the DDW-swollen state. Thereafter, the hydrogel granules were freeze-dried, and sterilized with ethylene oxide gas. The water content of gelatin hydrogel granules (the weight ratio of water present in the hydrogel to the wet hydrogel) was 96 wt.%, calculated from the hydrogel weight before and after swelling in phosphate-buffered saline solution (PBS, pH 7.4) for 24 h at 37 °C.

2.2. In vitro degradation assay

To evaluate the pattern of hydrogel degradation, the gelatin hydrogel granules were agitated in two types of degradation solution (1 ml): PBS with or without 10 μg ml^{-1} of collagenase (collagenase 1A, Nitta Gelatin Inc.) at 37 °C. At different time intervals, the solution supernatant was removed and replaced with the same volume of fresh PBS solution with or without collagenase. The gelatin concentration in each supernatant was determined by optical density (OD) measurement at 260 nm by spectrometry (DU800, Beckman Coulter, CA, USA) to evaluate the time profile of hydrogel degradation. The experiment was performed independently for three samples at every sampling time.

2.3. Preparation of PRP and growth factor detection

BALB/c mice (8 weeks old; Shimizu Laboratory Animal Supply, Kyoto, Japan) were used. All animal experiments were approved by the Kyoto University Committee for Animal Experimentation. Briefly, 15 mice were anesthetized by the intraperitoneal injection of pentobarbital (somnopentyl, Kyoritsu Seiyaku, Tokyo, Japan) at a dose of 0.65 mg kg^{-1} body weight. PRP was prepared with a platelet-rich plasma kit (JP200; Japan Paramedic Co. Ltd, Tokyo, Japan) according to the method reported [39–41]. Briefly, animal bloods (10 ml) were collected into tubes containing acid-citrate-dextrose solution formula A (1:4 v/v) anticoagulant and centrifuged for 7 min at 450g and 4 °C. Next, the yellow plasma with the buffy coat was carefully transferred into a BD Vacutainer® tube (Becton Dickinson Co., NJ, USA), and then centrifuged for 5 min at 1600g and 4 °C. The platelet pellet was collected and the thrombolytic pellet in 1.0 ml of plasma was used as PRP while the supernatant provided platelet-poor plasma (PPP). Before and after the PRP preparation, an aliquot was taken out to count the number of platelets. The density of platelets in the PRP prepared was increased by a factor of five when compared with that of the original blood.

To activate PRP for the release of growth factors, the PRP prepared was mixed with $CaCl_2$ solution at concentrations of 0.4, 0.6, 0.8, 1, 2, 4, and 10 wt.% at a ratio of 7:1 by volume, and then left for 1 h at 37 °C. As controls, PRP was treated with mixed 2 wt.% $CaCl_2$ and thrombin solution or by a conventional freeze–thaw method [42–44]. Briefly, PRP was frozen by liquid nitrogen for 1 min, and then rapidly thawed at 25 °C. The process was repeated three times.

The amount of growth factors, i.e. PDGF-BB, VEGF, EGF, and TGF-β_1, released was determined with a Quantikine® enzyme-linked immunosorbent assay (ELISA) kit (R&D Systems, MN, USA). For TGF-β_1 ELISA, the samples were first treated with acid to lower the pH to 2.0 to denature latency-associated peptide to allow the detection of active TGF-β_1. The supernatant was adjusted to neutral pH before ELISA.

2.4. Evaluation of PDGF-BB desorption from gelatin hydrogel granules incorporating PGFM

To evaluate the extent of platelet growth factors impregnated into the gelatin hydrogel granules, the amount of growth factors desorbed from gelatin hydrogel granules incorporating PGFM with or without $CaCl_2$ treatment was measured. The PRP was incubated with $CaCl_2$ solution at different Ca^{2+} concentrations for 1 h at 37 °C

or treated with the freeze–thaw method three times. Then, 100 μl of treated and non-treated PRP was impregnated into 10 mg of freeze-dried gelatin hydrogel granules for 1 h at 37 °C. The gelatin hydrogel granules incorporating PGFM were placed in 1 ml of PBS, and incubated for 3 h at 37 °C. The amount of growth factors in each PBS sample was determined by the ELISA similarly. The percentage adsorption of growth factors to gelatin hydrogel granules was calculated by the following formula:

$$\text{percentage adsorption} = 100 - (\text{the amount of desorbed growth factor}/\text{the amount of impregnated growth factor} \times 100)$$

The experiment was performed independently three times for each granule.

2.5. Preparation of gelatin hydrogel granules incorporating mixed PRP-treated bFGF and PGFM

An aqueous solution of human recombinant bFGF with an IEP of 9.6 (10 mg ml^{-1}) was kindly supplied by Kaken Pharmaceutical (Tokyo, Japan). The original bFGF solution was diluted with physiological saline solution (Otsuka Pharmaceutical Co. Ltd, Tokyo, Japan) to give a solution concentration of 10 mg ml^{-1}. The aqueous solution containing 100 μg of bFGF (10 μl) and 100 μl of PGFM was dropped onto a freeze-dried gelatin hydrogel granule for impregnation of PGFM and bFGF into the granule. The bFGF and PGFM solutions were completely sorbed into the hydrogel granule by swelling at 37 °C for 1 h, because the solution volume was less than theoretically required for the equilibrated swelling of hydrogels. Similarly, empty gelatin hydrogels without bFGF were prepared by adding PBS to the solution.

2.6. Release test of bFGF from gelatin hydrogel granules incorporating mixed PGFM and bFGF

To evaluate the bFGF release from the gelatin hydrogel granules incorporating mixed PGFM and bFGF, the gelatin hydrogels incorporating mixed PGFM and radiolabeled-bFGF were incubated in two types of release solution (1 ml): PBS with and without 10 μg ml^{-1} of collagenase at 37 °C. After 6 h incubation in PBS, there was a change from PBS to PBS with collagenase. At different time intervals, the solution supernatant was removed and replaced with the same volume of fresh PBS solution with or without collagenase. In this experiment, the PRP was treated with 2 wt.% $CaCl_2$ solution for platelet activation, and bFGF was labeled with ^{125}I.

Basic FGF was radioiodinated with chloramine-T according to the method described by Greenwood et al. [45]. Briefly, 5 μl of $Na^{125}I$ was added to 200 μl of 0.5 mg ml^{-1} bFGF solution in 0.5 M potassium PBS (pH 7.5) containing 0.5 M sodium chloride. Then 0.2 mg ml^{-1} of chloramine-T in 0.5 M potassium PBS (pH 7.5) containing 0.5 M sodium chloride (100 μl) was added to the solution mixture. After agitation at room temperature for 2 min, 100 μl solution containing 0.4 mg of sodium metabisulfate was added to the reaction solution to stop the radioiodination. The reaction mixture was passed through an anionic exchange column to remove the uncoupled, free ^{125}I molecules from the ^{125}I-labeled bFGF.

The mixture of the aqueous solution containing 100 μg of ^{125}I labeled-bFGF (10 μl) and 100 μl of PGFM was impregnated into 10 mg of freeze-dried gelatin hydrogel granules for 1 h at 37 °C. The supernatant was sampled at scheduled times and the amounts of bFGF in each supernatant samples were determined by the γ-counter. The experiment was done independently three times for each granule.

2.7. Release test of PDGF-BB from gelatin hydrogel granules incorporating PGFM

To evaluate the platelet PDGF-BB release from the gelatin hydrogel granules incorporating PGFM, the gelatin hydrogels incorporating PGFM were incubated in two types of release solution (1 ml): PBS with and without 10 μg ml^{-1} of collagenase at 37 °C. After 12 h incubation in PBS, there was a change from PBS to PBS with collagenase. At different time intervals, the solution supernatant was removed and replaced with the same volume of fresh PBS solution with or without collagenase. In this experiment, the PRP was treated with 2 wt.% $CaCl_2$ solution for platelet activation, and 100 μl of treated PRP was impregnated into 10 mg of freeze-dried gelatin hydrogel granules for 1 h at 37 °C. The supernatant was sampled at scheduled times and the amounts of PDGF-BB in each supernatant samples were determined by the ELISA similarly. The experiment was done independently three times for each granule.

2.8. In vivo experiments

Hind limb ischemia was created in 8 week old male BALB/c mice. Briefly, after the mice were anesthetized by an intraperitoneal pentobarbital (0.65 mg kg^{-1}) injection, the right groin area was shaved. The entire right saphenous artery and vein, right external iliac artery and vein, and deep femoral and circumflex arteries and vein were ligated, cut, and excised to obtain a murine model of severe hind limb ischemia. The BALB/c mice treated were randomly classified into six groups (n = 10 per group): hydrogel granules incorporating mixed PGFM and bFGF (PGFM + bFGF), gelatin hydrogel granules incorporating either PGFM or bFGF (PGFM or bFGF), gelatin hydrogel granules incorporating PPP (PPP), no treatment (NT), and PGFM- and bFGF-free PBS (PBS). All drugs were homogeneously injected into five sites in the thigh muscle of mouse ischemic hind limb by using a 27-gauge needle.

The animals were re-anesthetized by an intraperitoneal injection of pentobarbital (0.65 mg kg^{-1}) 1 week after treatment, and the following measurements were performed to evaluate the in vivo angiogenesis. Each experiment was done three times independently unless otherwise stated.

2.9. Hind limb blood perfusion

Hind limb blood perfusion was assessed by using a laser Doppler blood perfusion image (LDPI) analyzer (moorLDI™, Moor Instruments, Devon, UK) 1 week after treatment [14]. To evaluate the influence of surgical procedure on the blood flow, the blood perfusion of the normal hind limb and the treated one were measured with LDPI. To minimize external influence, such as light and temperature, the perfusion result was expressed as the LDPI index, which is the ratio of the blood perfusion in the right (ischemic) limb to that in the left (non-ischemic) limb of the same mouse [14,18,46]. The blood flow was measured in the site of vascular resection.

2.10. Histological examination

The specimens of muscular tissues were fixed with 4 wt.% paraformaldehyde (PFA) in 0.1 M phosphate-buffered solution overnight at 4 °C and then decalcified with Plank–Rychlo's solution overnight at room temperature. After decalcification, the samples were embedded in paraffin. Each specimen was cut into slices of the thigh, 4 μm thick in cross-section. For histological analysis, the section was stained with hematoxylin and eosin (HE) dyes, and the number of blood vessels newly formed in the thigh was counted in a blind fashion. The ratio of blood vessels newly formed

in the right (ischemic) limb to those in the left (non-ischemic) limb of the same mouse was calculated.

2.11. Immunohistological analysis

The animals were re-anesthetized by an intraperitoneal injection of pentobarbital (0.65 mg kg^{-1}) 1 week after treatment, and the mice were perfusion-fixed with 4 wt.% PFA solution. The ischemic thigh was decalcified and embedded in paraffin. Paraffin sections (5 μm thick) of tissues were stained with a mouse monoclonal anti-α-smooth muscle actin antibody (α-SMA; Sigma–Aldrich Japan K.K., Tokyo, Japan). From each mouse, all fields on tissue sections were photographed with a digital camera (Olympus, Tokyo, Japan). The number of α-SMA (vascular smooth muscle marker)-positive vessels was counted in a blind fashion. The number of blood vessels was counted for the HE staining section. The percentage of α-SMA-positive blood vessels to that of total blood vessels was calculated. Each experiment was done three times independently.

2.12. Statistical analysis

All the statistical data were expressed as the mean ± standard error of the mean. The data were analyzed by ANOVA to determine the statistical significance between the two mean values. *P* values less than 0.05 were considered to be significant.

3. Results

3.1. $CaCl_2$ treatment of PRP for the release of platelet growth factors

Table 1 shows the concentration of various growth factors released from PRP after the freeze–thaw treatment. The treatment activated the platelet of PRP to release various growth factors. Based on the profile of growth factors released, PDGF-BB, VEGF, EGF, and TGF-β_1 were selected as representative platelet growth factors because these were produced in the largest amounts and showed the greatest ability to enhance the maturation of newly formed blood vessels [38,47–53].

Fig. 1 shows the concentration of PDGF-BB released from PRP after the $CaCl_2$ treatment. Upon treating with 0.8, 1, 2, and 4 wt.% $CaCl_2$ solution, the concentration of PDGF-BB in the soluble fraction of PRP was significantly higher compared with that of non-treated PRP. On the other hand, treatment with 10 wt.% $CaCl_2$ solution did not increase the PDGF-BB amount. The concentration of EGF in the soluble fraction of PRP was significantly higher compared with the non-treated PRP and the 10 wt.% $CaCl_2$ solution treated PRP (Fig. 2A). The amount of VEGF extracted from PRP was higher in PRP treated with $CaCl_2$ compared with that of non-treatment (Fig. 2B). In this study, PDGF is highlighted because it has the ability to enhance the maturation of blood vessels. In addition, PDGF is one of the main factors present in PRP. However, the amount of TGF-β_1 in PRP treated with 1, 2, and 4 wt.% $CaCl_2$ was higher than that of 10 wt.% $CaCl_2$ treated PRP, although the difference was not significant (Fig. 2C).

Table 1
Concentration of growth factors in PRP.

Growth factor	Concentration (pg/ml)
PDGF-BB	9440 ± 1620
VEGF	2040 ± 971
TGF-β_1	30,500 ± 20,500
EGF	906 ± 206
bFGF	32.6 ± 8.7

The growth factors were extracted from PRP through the freeze- and thaw treatment.

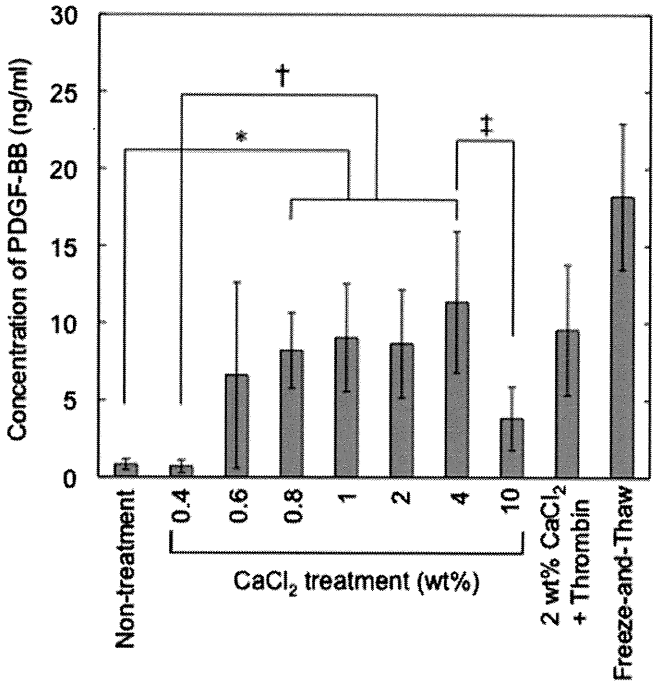

Fig. 1. Concentration of PDGF-BB released from PRP after treatment with $CaCl_2$ solution at different Ca^{2+} concentrations, a mixed solution of 2 wt.% $CaCl_2$ and thrombin, and freeze–thaw treatment. $^*P < 0.05$, significantly different from the values of non-treated PRP. $^\dagger P < 0.05$, significantly different from the values of 0.4 wt.% $CaCl_2$-treated PRP. $^\ddagger P < 0.05$, significantly different from the values of 10 wt.% $CaCl_2$-treated PRP.

3.2. Adsorption of growth factors to gelatin hydrogel granules incorporating PGFM and the in vitro profiles of PDGF-BB release

Fig. 3 shows the adsorption patterns of growth factors to gelatin hydrogel granules incorporating PGFM. For PRP treated with 0.8, 1, 2, and 4 wt.% $CaCl_2$ for 1 h at 37 °C, the amount of PDGF-BB adsorption was significantly lower compared with that treated with 0.4 and 0.6 wt.% $CaCl_2$ (Fig. 3A). The pattern of VEGF, EGF, and TGF-β_1 adsorption from the hydrogel granules incorporating PGFM was influenced by the $CaCl_2$ concentration (Fig. 3B–D). On the other hand, Fig. 4 shows the adsorption patterns of growth factors to gelatin hydrogel granules incorporating mixed PGFM and bFGF and time courses of bFGF from gelatin hydrogel granules incorporating mixed PGFM and bFGF in PBS with or without collagenase. When mixed PGFM and bFGF were impregnated into gelatin hydrogel granules, the adsorption rate of bFGF to gelatin hydrogel granules was ~50% of impregnated bFGF (Fig. 4A). In the release in PBS, ~60% of bFGF was released from the hydrogel granules. When mixed PGFM and bFGF were impregnated to gelatin hydrogel granules, the initial burst of bFGF was increased compared with that of a single impregnation of bFGF. However, when the release test was performed in PBS containing collagenase, the bFGF was released with time (Fig. 4B).

Fig. 5 shows the time courses of PDGF-BB from gelatin hydrogel granules incorporating PRP treated with 2 wt.% $CaCl_2$ solution in PBS with or without collagenase. In the release in PBS, PDGF-BB was not released from the hydrogel granules, although an initial burst of small amounts released was observed. However, when the release test was performed in PBS containing collagenase, the PDGF-BB was released with time. A similar addition effect of collagenase on the time profile of hydrogel degradation was seen. A

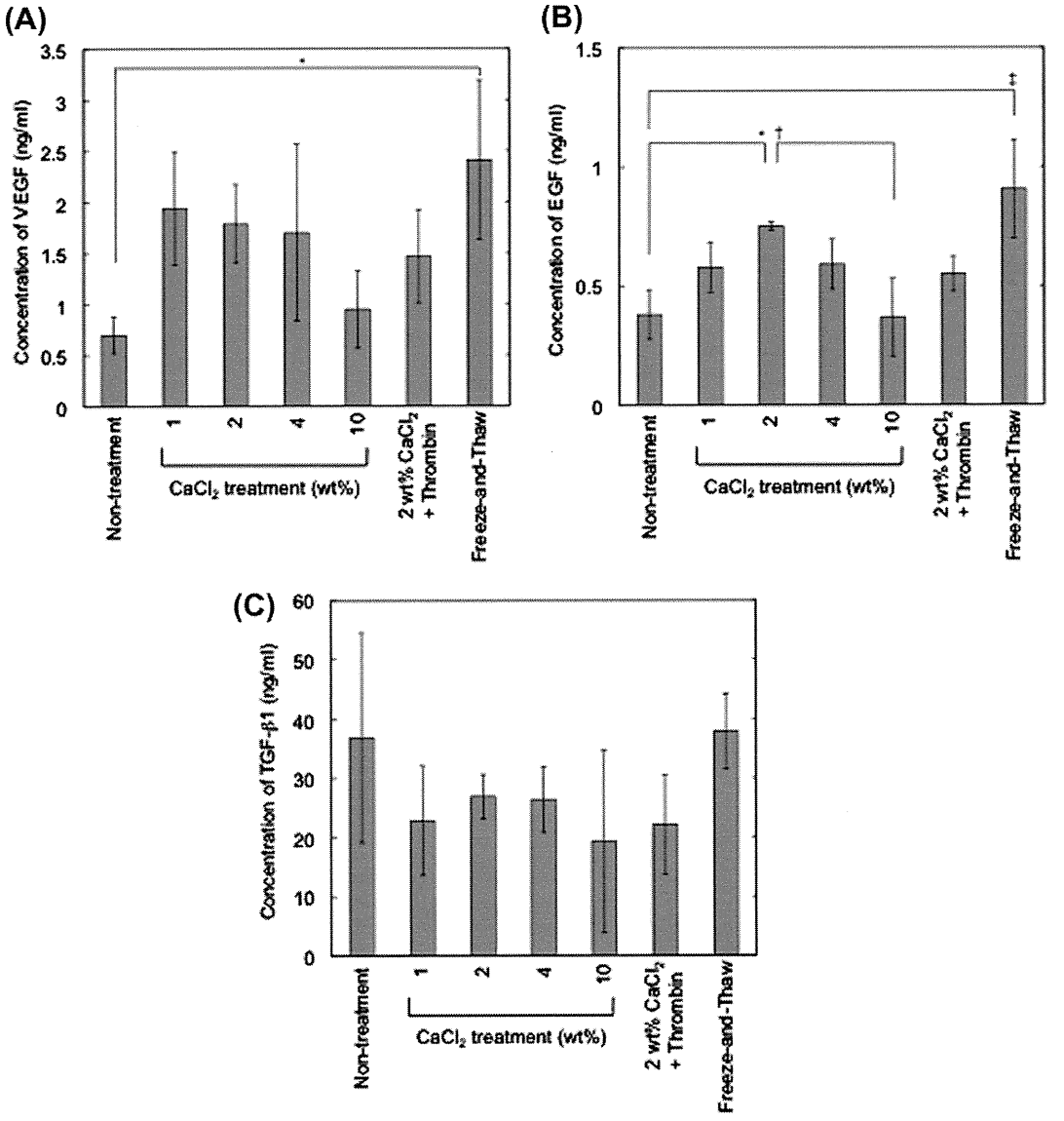

Fig. 2. Concentration of growth factors released from PRP after treatment with $CaCl_2$ solution at different Ca^{2+} concentrations, a mixed solution of 2 wt.% $CaCl_2$ and thrombin, and freeze–thaw treatment. (A) Concentration of EGF released from PRP. $^*P < 0.05$, significantly different from the values of non-treated PRP. $^\dagger P < 0.05$, significantly different from the values of 10 wt.% $CaCl_2$-treated PRP. $^\ddagger P < 0.05$; significantly different from the values of freeze–thaw-treated PRP. (B) Concentration of VEGF released from PRP. $^*P < 0.05$, significantly different from the values of freeze–thaw-treated PRP. (C) Concentration of TGF-β_1 released from PRP.

good correlation of time profiles was observed between the PDGF-BB release and the hydrogel degradation.

3.3. Angiogenic effects of gelatin hydrogel granules incorporating mixed PGFM and bFGF

Fig. 6 shows the in vivo angiogenic effects of gelatin hydrogel granules incorporating PGFM with or without bFGF combination 1 week after implantation. The PRP was treated with 2 wt.% $CaCl_2$ solution. From the histological sections, new formation of blood vessels was observed for the hydrogel granules incorporating mixed PGFM and bFGF. The number of blood vessels newly formed was significantly higher compared with that of other groups. The number of vessels was not increased by injection of hydrogel granules incorporating PGFM, bFGF, or PBS. PBS solution containing PGFM, bFGF, or mixed PGFM and bFGF did not increase the number of new blood vessels (data not shown). The percentage of α-SMA-positive blood vessels was increased due to the granules incorporating mixed PGFM and bFGF to a significantly greater extent compared with that of other controls. No difference in the number of vessels between the right and left limbs was observed for either the non-treated group or the group injected with empty granules. This indicates that neither the surgical procedure nor the granule injection induced angiogenesis.

Fig. 7 shows blood perfusion levels in the ischemic limb after the injection of a range of gelatin hydrogel granules incorporating mixed PGFM and bFGF. The injection of hydrogel granules incorporating mixed PGFM and bFGF significantly enhanced the perfusion index, in marked contrast to that of other groups.

4. Discussion

The present study demonstrates that the multiple releases of PRP growth factors and bFGF from gelatin hydrogel granules was effective in increasing the number of newly formed blood vessels and the blood flow level in the ischemic legs. In addition, the number of α-SMA-positive blood vessels was also increased, which suggests the maturation of blood vessels was enhanced.

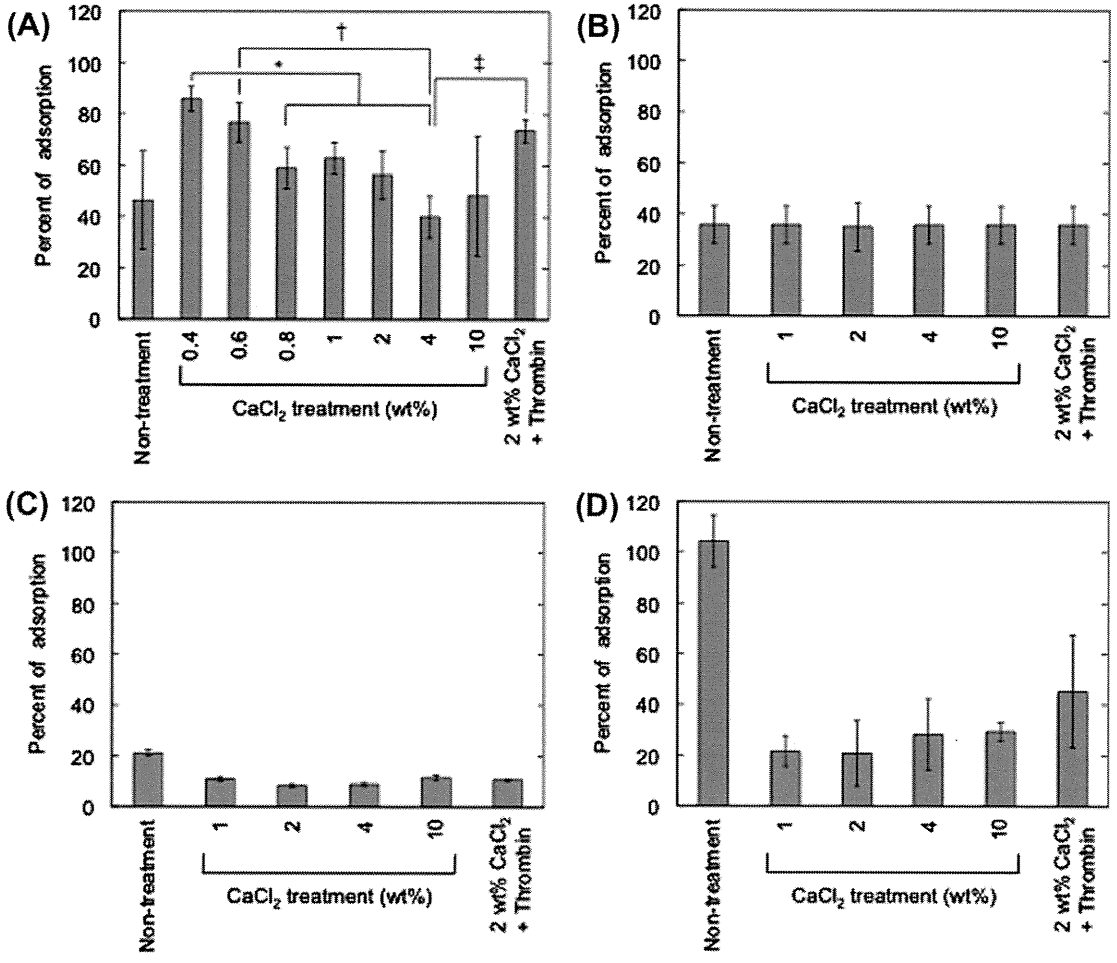

Fig. 3. Adsorption of growth factors to gelatin hydrogel granules. After treatment of $CaCl_2$ solution at different Ca^{2+} concentrations and a mixed solution of 2 wt.% $CaCl_2$ and thrombin, the PRP-treated growth factor was incorporated into the gelatin hydrogels at 37 °C for 1 h. The concentration of growth factors desorbed from gelatin hydrogel granules incorporating PGFM treated was detected by ELISA. (A) The percentage adsorption of PDGF-BB to gelatin hydrogel. $^*P < 0.05$, significantly different from the values of 0.4 wt.% $CaCl_2$-treated PRP. $^\dagger P < 0.05$, significantly different from the values of 0.6 wt.% $CaCl_2$-treated PRP. $^\ddagger P < 0.05$, significantly different from the values of the mixed solution of 2 wt.% $CaCl_2$ and thrombin. (B) The percentage adsorption of VEGF to gelatin hydrogel. (C) The percentage adsorption of EGF to gelatin hydrogel. (D) The percentage adsorption of TGF-β_1 to gelatin hydrogel.

In the living tissue, it is well known that various growth factors interact with the components of extracellular matrix, such as acidic polysaccharides and collagen, through various intermolecular interaction forces [54]. In addition, the physicochemical interactions serve to maintain and enhance the in vivo biological function of growth factors. For instance, bFGF with an IEP of 9.6 forms polyion complexes with heparin and heparan sulfate in vivo, resulting in the stabilization and regulation of biological activities [43,55]. The manner of natural physicochemical interactions provides a good example for the design of the controlled release system of growth factors. Based on this, we have developed biodegradable hydrogels of gelatin [9–11,56]. The physicochemical properties of gelatin, such as its electric nature, can be readily modified by the preparation procedure. For example, gelatin prepared via an alkaline process from collagen has an IEP of 5.0 and is negatively charged at the physiological pH, whereas an acidic process gives a positively charged gelatin with an IEP of 9.0. This behavior of gelatin can be used to tailor electrostatic interactions with growth factors of different IEPs [56]. Recently, human recombinant growth factors have become commercially available and have been experimentally or clinically used for tissue regeneration applications. However, when the growth factor in solution form is used in vivo, biological activity is not always expected. This is because it is unstable in vivo due to rapid enzymatic digestion or deactivation. Therefore, delivery technology is essential to enable the growth factor to efficiently enhance the biological functions. We have succeeded in the controlled release of various growth factors as well as PRP from the gelatin hydrogels [6–13]. It has been recognized that, when activated, the platelets of PRP release various growth factors through the degranulation of α granules and the factors released exhibit various biological activities [23]. For example, collagen and thrombin trigger platelet aggregation and the subsequent release of platelet growth factors [57]. It has been experimentally confirmed that the gelatin of a denatured collagen can function to trigger the platelet activation for growth factor release [36]. When impregnated into freeze-dried hydrogel, it is likely that the PRP is activated by the contact with gelatin molecules to release the growth factors. The factors released interact with gelatin molecules during the impregnation procedure. Consequently, the PRP growth factors can be released from the gelatin hydrogels as a result of hydrogel degradation. However, the contact of PRP with gelatin molecules is not always strong enough to release the PRP growth factors. In this study, the treatment of PRP with $CaCl_2$ solution was used in an attempt to accelerate the release of PRP growth factors. $CaCl_2$ treatment is one of the well-known methods used to activate PRP [41,58].

The adsorption experiment demonstrated that the percentage of PRP growth factors desorbed increased with decrease in the

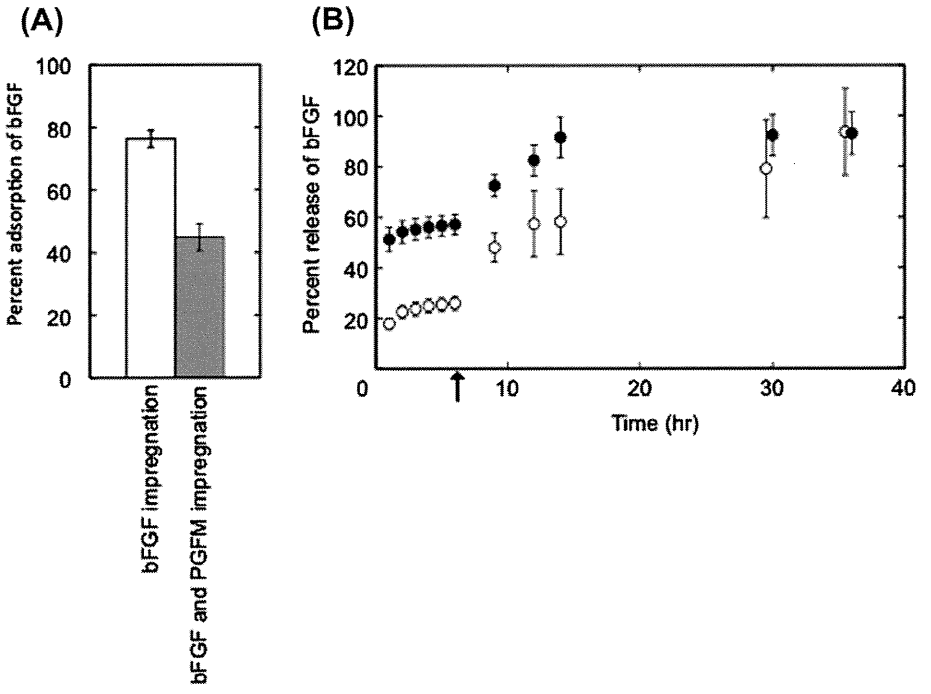

Fig. 4. Adsorption of bFGF to gelatin hydrogel granules and time course of bFGF release from gelatin hydrogel granules incorporating mixed PGFM and ^{125}I-labeled bFGF. (A) The percentage adsorption of bFGF to gelatin hydrogel. (B) The time course of bFGF release from gelatin hydrogel granules incorporating mixed PGFM and ^{125}I-labeled bFGF (○) and gelatin hydrogel granules incorporating ^{125}I-labeled bFGF (●) in PBS with or without collagenase. The PBS solution was changed to that with collagenase at the time indicated with an arrow.

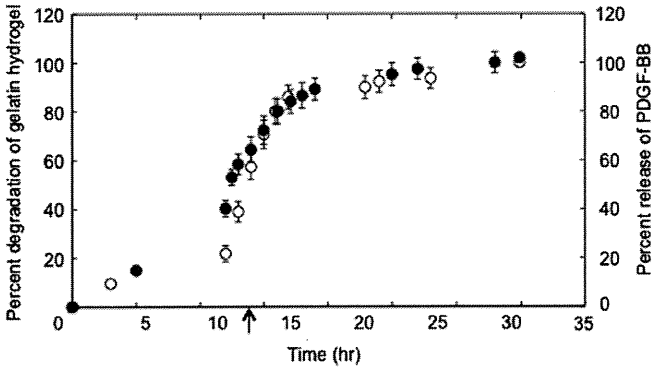

Fig. 5. The time course of PDGF-BB release from gelatin hydrogel granules incorporating PRP treated with 2 wt.% $CaCl_2$ solution (○) and hydrogel degradation (●) in PBS with or without collagenase. The PBS solution was changed to that with collagenase at the time indicated with an arrow.

$CaCl_2$ concentration. This can be explained in terms of solution ionic strength. It is recognized that the growth factor physicochemically interacts with the gelatin molecules of hydrogels while one of the main interactions is electrostatic. It is likely, therefore, that the increased $CaCl_2$ concentration suppresses the interaction between the PRP growth factor and gelatin molecules, resulting in an increase in the desorption percentage. In addition, the pattern of PDGF-BB release from the hydrogel granules incorporating PGFM is influenced by the $CaCl_2$ concentration. When the concentration was 4 wt.%, a higher amount of PDGF-BB release for the initial time period was observed compared with that of granules incorporating PGFM treated with 2 wt.% $CaCl_2$ solution. Hence, the $CaCl_2$ concentration for PRP treatment was fixed at 2 wt.%. The time profile of PDGF-BB release from the granules incorporating 2 wt.% $CaCl_2$ treated-PRP was in good accordance with that of granule degradation. This indicates that growth factor release is based on the degradation of release carrier hydrogels. When PRP was treated with the freeze–thaw method, the concentration of PDGF-BB in the soluble fraction of PRP was significantly higher compared with that of $CaCl_2$-treated PRP. However, the activation of PRP by the freeze–thaw method is not always suitable as it is a complex process to use in clinical settings.

The $CaCl_2$ treatment affects the amount of platelet growth factor released and the adsorption profile to the hydrogel granules incorporating PGFM (Figs. 1 and 2). In this study, PDGF-BB, VEGF, EGF, and TGF-β_1 were selected as representative platelet growth factors because these were produced in the largest amounts and showed the greatest ability to enhance the maturation of newly formed blood vessels [47–49,51,53,59]. With $CaCl_2$ concentrations of 1, 2, and 4 wt.%, the amount of growth factors was higher than that of higher or lower $CaCl_2$ concentrations. The treatment at the lower concentration would not be enough to activate the platelets. On the other hand, it is possible that the strong activation of platelets with higher concentrations of $CaCl_2$ solution results in the release of platelet ingredients. The ingredients may suppress the activity of platelet growth factor.

We have demonstrated successful angiogenic effects on ischemic legs and hearts by biodegradable acidic gelatin hydrogels for the controlled release of bFGF [10,11]. The bFGF release from the gelatin hydrogels was therapeutically effective in various animal models (i.e. either non-diabetic or diabetic) for acute myocardial infarction, prevascularization for cardiomyocyte transplantation to the ischemic heart, limb ischemia, and bone regeneration of sternum [14–21]. In the release system, both the biodegradable gelatin hydrogels of the release carrier and the bFGF of an angiogenic factor are clinically available at present. Based on the results of animal experiments, several clinical trials have been started to confirm the safety and feasibility of bFGF release from the gelatin hydrogel in patients with clinical limb ischemia. Using gelatin hydrogels for bFGF release is simple, safe, and effective from the clinical viewpoint. It is not necessary to use genetic materials and collect cells to be transplanted. In addition, no elevation of

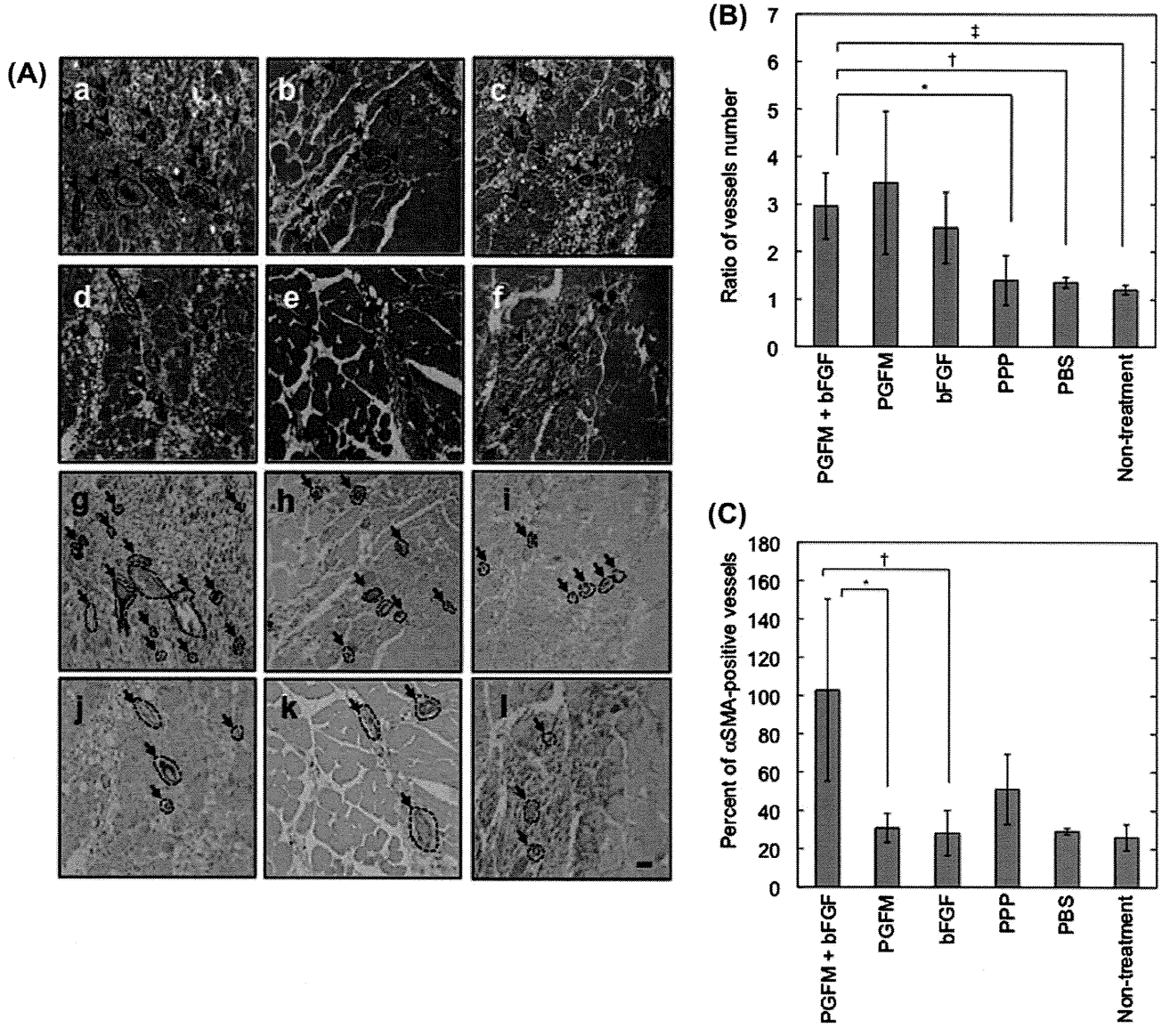

Fig. 6. In vivo angiogenic effects of gelatin hydrogel granules incorporating PRP with or without bFGF 1 week after implantation. (A) Histological section ((a–f) hematoxylin and eosin and (g–l) anti-α-SMA immunohistochemical staining) of tissues injected with different gelatin hydrogel granules: hydrogels incorporating (a, g) PGFM and bFGF, (b, h) PGFM, (c, i) bFGF, (d, j) PPP, or (e, k) PBS, and (f, l) non-treatment. The scale bar indicates 100 μm. (B) The number ratio of blood vessels newly formed around tissues injected with gelatin hydrogel granules. The number ratio of blood vessels newly formed in the right (ischemic) limb was calculated as for that in the left (non-ischemic) limb of the same mouse. A ratio of 1.0 was calculated in non-treated mice. $^{*}P < 0.05$, significantly different from the value of gelatin hydrogel granules incorporating PPP. $^{\dagger}P < 0.01$, significantly different from the value of gelatin hydrogel granules incorporating PBS. $^{\ddagger}P < 0.01$, significantly different from the non-treatment value. (C) Percentage of anti-α-SMA-positive blood vessels around the tissue injected with gelatin hydrogel granules. The percentage of number of α-SMA-positive blood vessels to that of total blood vessels was calculated. $^{*}P < 0.05$, significantly different from the value of gelatin hydrogel granules incorporating PGFM. $^{\dagger}P < 0.05$, significantly different from the value of gelatin hydrogel granules incorporating bFGF.

bFGF serum level was reported clinically [22]. However, the bFGF release system has some room for improvement for clinical applications. In practical terms, it is suitable for the treatment of patients with severe conditions to enhance the number of newly formed blood vessels and their biological maturation. The enhancement of blood vessel maturation is one of the practical strategies used to treat such patients with severe conditions. Research on the maturation of blood vessels in terms of growth factor usage has been reported. PRP is a source of autologous growth factors, including PDGF-BB, VEGF, EGF, and TGF-β. Several growth factors become intricately involved in angiogenesis. The PDGF-BB, VEGF, and TGF-β play an important role as proangiogenic stimulators. Several studies reported that PDGF-BB has a potent arteriogenic effect that promotes differentiation of endothelial cells [60], VEGF is known to stimulate angiogenesis after ischemia [61], and TGF-β promotes cell mitosis [53]. However, other studies indicated that several growth factors, such as PDGF-BB and TGF-β, inhibit the angiogenic effect of bFGF [62–65]. These studies evaluated the angiogenic effect using mixed solutions of growth factors. Moreover, the amounts of growth factors were used transiently at high concentration. On the other hand, we used gelatin hydrogel granules incorporating PGFM and bFGF in this study; these gelatin hydrogel granules were degraded for 2 weeks, and sustained release of the encapsulated growth factors occurred. Thus, our sustained-release system and previous reports are fundamentally different. Among the growth factors, PDGF-BB is one of the most powerful, allowing blood vessels to mature functionally [38,49]. This finding suggests that multiple releases of PGFM and bFGF will enhance the maturation of blood vessels. Mooney et al. reported that the dual release of VEGF and PDGF enhanced the maturation

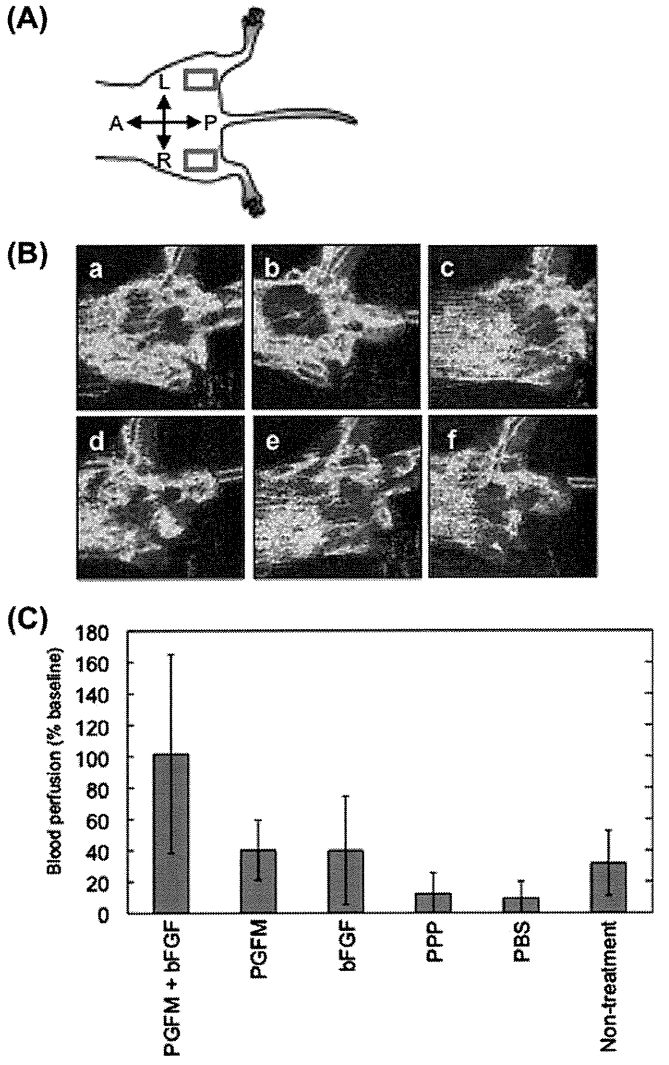

Fig. 7. In vivo blood perfusion effects of gelatin hydrogel granules incorporating PGFM with or without bFGF 1 week after implantation. (A) Dorsal view of mouse image. The blood flow was measured in boxed area. (B) The image of laser Doppler perfusion of tissues injected with different gelatin hydrogel granules. (a) Hydrogels incorporating PGFM and bFGF, (b) PGFM, (c, i) bFGF, (d) PPP or (e) PBS, and (f) non-treatment. (C) The percentage of blood perfusion in the newly formed blood vessels around the tissue injected with gelatin hydrogel granules. The percentage of blood perfusion in the right (ischemic) limb was calculated as for that in the left (non-ischemic) limb of the same mouse. The baseline is the perfusion index of non-ischemic limb.

of newly formed blood vessels compared with that of single VEGF release. The in vivo experiments clearly indicate that the dual release of PRP-treated PGFM and bFGF from the biodegradable gelatin hydrogel granules promoted not only angiogenesis in a mouse model of limb ischemia, but also the maturation of blood vessels whereas the release of either PGFM or bFGF was not effective. There have been reports on the synergistic effects of different drugs on the enhancement of tissue regeneration [66–68] and tissue maturation. The dual release technology is available for any type of drug and is able to promote the regeneration of various tissues.

Appendix A. Figures with essential colour discrimination

Certain figures in this article, particularly Figures 6 and 7, are difficult to interpret in black and white. The full colour images can be found in the on-line version, at doi:10.1016/j.actbio.2012.01.016.

References

[1] Blau H, Khavari P. Gene therapy: progress, problems, prospects. Nat Med 1997;3(6):612–3.
[2] Chuah MK, Collen D, VandenDriessche T. Biosafety of adenoviral vectors. Curr Gene Ther 2003;3(6):527–43.
[3] Howe SJ, Mansour MR, Schwarzwaelder K, Bartholomae C, Hubank M, Kempski H, et al. Insertional mutagenesis combined with acquired somatic mutations causes leukemogenesis following gene therapy of SCID-X1 patients. J Clin Invest 2008;118(9):3143–50.
[4] Kai S, Hara H. Allogeneic hematopoietic stem cell transplantation. Ther Apher Dial 2003;7(3):285–91.
[5] Steward CG, Jarisch A. Haemopoietic stem cell transplantation for genetic disorders. Arch Dis Child 2005;90(12):1259–63.
[6] Ozeki M, Tabata Y. Promoted growth of murine hair follicles through controlled release of basic fibroblast growth factor. Tissue Eng 2002;8(3):359–66.
[7] Hong L, Tabata Y, Miyamoto S, Yamamoto M, Yamada K, Hashimoto N, et al. Bone regeneration at rabbit skull defects treated with transforming growth factor-beta1 incorporated into hydrogels with different levels of biodegradability. J Neurosurg 2000;92(2):315–25.
[8] Kanematsu A, Yamamoto S, Ozeki M, Noguchi T, Kanatani I, Ogawa O, et al. Collagenous matrices as release carriers of exogenous growth factors. Biomaterials 2004;25(18):4513–20.
[9] Yamamoto M, Takahashi Y, Tabata Y. Enhanced bone regeneration at a segmental bone defect by controlled release of bone morphogenetic protein-2 from a biodegradable hydrogel. Tissue Eng 2006;12(5):1305–11.
[10] Tabata Y, Hijikata S, Ikada Y. Enhanced vascularization and tissue granulation by basic fibroblast growth factor impregnated in gelatin hydrogels. J Control Release 1994;31(2):189–99.
[11] Tabata Y, Hijikata S, Muniruzzaman M, Ikada Y. Neovascularization effect of biodegradable gelatin microspheres incorporating basic fibroblast growth factor. J Biomater Sci Polym Ed 1999;10(1):79–94.
[12] Ozeki M, Tabata Y. Affinity evaluation of gelatin for hepatocyte growth factor of different types to design the release carrier. J Biomater Sci Polym Ed 2006;17(1–2):139–50.
[13] Sakaguchi G, Tambara K, Sakakibara Y, Ozeki M, Yamamoto M, Premaratne G, et al. Control-released hepatocyte growth factor prevents the progression of heart failure in stroke-prone spontaneously hypertensive rats. Ann Thorac Surg 2005;79(5):1627–34.
[14] Arai Y, Fujita M, Marui A, Hirose K, Sakaguchi H, Ikeda T, et al. Combined treatment with sustained-release basic fibroblast growth factor and heparin enhances neovascularization in hypercholesterolemic mouse hindlimb ischemia. Circ J 2007;71(3):412–7.
[15] Hirose K, Fujita M, Marui A, Arai Y, Sakaguchi H, Huang Y, et al. Combined treatment of sustained-release basic fibroblast growth factor and sarpogrelate enhances collateral blood flow effectively in rabbit hindlimb ischemia. Circ J 2006;70(9):1190–4.
[16] Hirose K, Marui A, Arai Y, Fujita M, Nomura T, Mitsuyama M, et al. Sustained-release form of basic fibroblast growth factor prevents catheter-related bacterial invasion in mice. Interact Cardiovasc Thorac Surg 2005;4(6):526–30.
[17] Iwakura A, Tabata Y, Tamura N, Doi K, Nishimura K, Nakamura T, et al. Gelatin sheet incorporating basic fibroblast growth factor enhances healing of devascularized sternum in diabetic rats. Circulation 2001;104(12 Suppl 1):I325–9.
[18] Marui A, Kanematsu A, Yamahara K, Doi K, Kushibiki T, Yamamoto M, et al. Simultaneous application of basic fibroblast growth factor and hepatocyte growth factor to enhance the blood vessels formation. J Vasc Surg 2005;41(1):82–90.
[19] Sakakibara Y, Nishimura K, Tambara K, Yamamoto M, Lu F, Tabata Y, et al. Prevascularization with gelatin microspheres containing basic fibroblast growth factor enhances the benefits of cardiomyocyte transplantation. J Thorac Cardiovasc Surg 2002;124(1):50–6.
[20] Takaba K, Jiang C, Nemoto S, Saji Y, Ikeda T, Urayama S, et al. A combination of omental flap and growth factor therapy induces arteriogenesis and increases myocardial perfusion in chronic myocardial ischemia: evolving concept of biologic coronary artery bypass grafting. J Thorac Cardiovasc Surg 2006;132(4):891–9.
[21] Tambara K, Premaratne GU, Sakaguchi G, Kanemitsu N, Lin X, Nakajima H, et al. Administration of control-released hepatocyte growth factor enhances the efficacy of skeletal myoblast transplantation in rat infarcted hearts by greatly increasing both quantity and quality of the graft. Circulation 2005;112(9 Suppl):I129–134.
[22] Marui A, Tabata Y, Kojima S, Yamamoto M, Tambara K, Nishina T, et al. A novel approach to therapeutic angiogenesis for patients with critical limb ischemia by sustained release of basic fibroblast growth factor using biodegradable gelatin hydrogel: an initial report of the phase I-IIa study. Circ J 2007;71(8):1181–6.
[23] Marx RE. Platelet-rich plasma: evidence to support its use. J Oral Maxillofac Surg 2004;62(4):489–96.
[24] Margolis DJ, Kantor J, Santanna J, Strom BL, Berlin JA. Effectiveness of platelet releasate for the treatment of diabetic neuropathic foot ulcers. Diabetes Care 2001;24(3):483–8.
[25] Hokugo A, Sawada Y, Hokugo R, Iwamura H, Kobuchi M, Kambara T, et al. Controlled release of platelet growth factors enhances bone regeneration at rabbit calvaria. Oral Surg Oral Med Oral Pathol Oral Radiol Endod 2007;104(1):44–8.

[26] Marx RE, Carlson ER, Eichstaedt RM, Schimmele SR, Strauss JE, Georgeff KR. Platelet-rich plasma: growth factor enhancement for bone grafts. Oral Surg Oral Med Oral Pathol Oral Radiol Endod 1998;85(6):638–46.
[27] Bhanot S, Alex JC. Current applications of platelet gels in facial plastic surgery. Facial Plast Surg 2002;18(1):27–33.
[28] Man D, Plosker H, Winland-Brown JE. The use of autologous platelet-rich plasma (platelet gel) and autologous platelet-poor plasma (fibrin glue) in cosmetic surgery. Plast Reconstr Surg 2001;107(1):229–37. Discussion 229–238.
[29] Hee HT, Majd ME, Holt RT, Myers L. Do autologous growth factors enhance transforaminal lumbar interbody fusion? Eur Spine J 2003;12(4):400–7.
[30] Bir SC, Esaki J, Marui A, Yamahara K, Tsubota H, Ikeda T, et al. Angiogenic properties of sustained release platelet-rich plasma: characterization in-vitro and in the ischemic hind limb of the mouse. J Vasc Surg 2009;50(4):870–9. e872.
[31] Ishida K, Kuroda R, Miwa M, Tabata Y, Hokugo A, Kawamoto T, et al. The regenerative effects of platelet-rich plasma on meniscal cells in vitro and its in vivo application with biodegradable gelatin hydrogel. Tissue Eng 2007;13(5):1103–12.
[32] Saito M, Takahashi KA, Arai Y, Inoue A, Sakao K, Tonomura H, et al. Intraarticular administration of platelet-rich plasma with biodegradable gelatin hydrogel microspheres prevents osteoarthritis progression in the rabbit knee. Clin Exp Rheumatol 2009;27(2):201–7.
[33] Nagae M, Ikeda T, Mikami Y, Hase H, Ozawa H, Matsuda K, et al. Intervertebral disc regeneration using platelet-rich plasma and biodegradable gelatin hydrogel microspheres. Tissue Eng 2007;13(1):147–58.
[34] Okamoto SI, Ikeda T, Sawamura K, Nagae M, Hase H, Mikami Y, et al. Positive effect on bone fusion by the combination of platelet-rich plasma and a gelatin beta-tricalcium phosphate sponge: a study using a posterolateral fusion model of lumbar vertebrae in rats. Tissue Eng Part A 2012;18(1–2):157–66.
[35] Sawamura K, Ikeda T, Nagae M, Okamoto S, Mikami Y, Hase H, et al. Characterization of in vivo effects of platelet-rich plasma and biodegradable gelatin hydrogel microspheres on degenerated intervertebral discs. Tissue Eng Part A 2009;15(12):3719–27.
[36] Hokugo A, Ozeki M, Kawakami O, Sugimoto K, Mushimoto K, Morita S, et al. Augmented bone regeneration activity of platelet-rich plasma by biodegradable gelatin hydrogel. Tissue Eng 2005;11(7–8):1224–33.
[37] Jain RK. Molecular regulation of vessel maturation. Nat Med 2003;9(6):685–93.
[38] Zymek P, Bujak M, Chatila K, Cieslak A, Thakker G, Entman ML, et al. The role of platelet-derived growth factor signaling in healing myocardial infarcts. J Am Coll Cardiol 2006;48(11):2315–23.
[39] Aghaloo TL, Moy PK, Freymiller EG. Investigation of platelet-rich plasma in rabbit cranial defects: a pilot study. J Oral Maxillofac Surg 2002;60(10):1176–81.
[40] Kazakos K, Lyras DN, Thomaidis V, Agrogiannis G, Botaitis S, Drosos G, et al. Application of PRP gel alone or in combination with guided bone regeneration does not enhance bone healing process: an experimental study in rabbits. J Craniomaxillofac Surg 2011;39(1):49–53.
[41] Marukawa E, Oshina H, Iino G, Morita K, Omura K. Reduction of bone resorption by the application of platelet-rich plasma (PRP) in bone grafting of the alveolar cleft. J Craniomaxillofac Surg 2011;39(4):278–83.
[42] Doucet C, Ernou I, Zhang Y, Llense JR, Begot L, Holy X, et al. Platelet lysates promote mesenchymal stem cell expansion: a safety substitute for animal serum in cell-based therapy applications. J Cell Physiol 2005;205(2):228–36.
[43] Rifkin DB, Moscatelli D. Recent developments in the cell biology of basic fibroblast growth factor. J Cell Biol 1989;109(1):1–6.
[44] Schallmoser K, Strunk D. Preparation of pooled human platelet lysate (pHPL) as an efficient supplement for animal serum-free human stem cell cultures. J Vis Exp 2009;32:e1523.
[45] Greenwood FC, Hunter WM, Gglover TC. The preparation of I-labeled human growth hormone of high specific radioactivity. Biochem J 1963;89:114.
[46] Couffinhal T, Silver M, Zheng LP, Kearney M, Witzenbichler B, Isner JM. Mouse model of angiogenesis. Am J Pathol 1998;152(6):1667–79.
[47] Bertrand-Duchesne MP, Grenier D, Gagnon G. Epidermal growth factor released from platelet-rich plasma promotes endothelial cell proliferation in vitro. J Periodontal Res 2010;45(1):87–93.
[48] Gospodarowicz D, Greenburg G, Bialecki H, Zetter BR. Factors involved in the modulation of cell proliferation in vivo and in vitro: the role of fibroblast and epidermal growth factors in the proliferative response of mammalian cells. In Vitro 1978;14(1):85–118.
[49] Hellberg C, Ostman A, Heldin CH. PDGF and vessel maturation. Recent Results Cancer Res 2010;180:103–14.
[50] Munoz-Chapuli R. Evolution of angiogenesis. Int J Dev Biol 2011;55(4–5):345–51.
[51] Nicosia RF, Nicosia SV, Smith M. Vascular endothelial growth factor, platelet-derived growth factor, and insulin-like growth factor-1 promote rat aortic angiogenesis in vitro. Am J Pathol 1994;145(5):1023–9.
[52] Ribatti D, Nico B, Crivellato E. The role of pericytes in angiogenesis. Int J Dev Biol 2011;55(3):261–8.
[53] Schultz GS, Grant MB. Neovascular growth factors. Eye (Lond) 1991;5(Pt 2):170–80.
[54] Taipale J, Keski-Oja J. Growth factors in the extracellular matrix. FASEB J 1997;11(1):51–9.
[55] Gospodarowicz D. Biological activities of fibroblast growth factors. Ann NY Acad Sci 1991;638(1):1–8.
[56] Yamamoto M, Ikada Y, Tabata Y. Controlled release of growth factors based on biodegradation of gelatin hydrogel. J Biomater Sci Polym Ed 2001;12(1):77–88.
[57] Kaplan KL, Nossel HL, Drillings M, Lesznik G. Radioimmunoassay of platelet factor 4 and beta-thromboglobulin: development and application to studies of platelet release in relation to fibrinopeptide A generation. Br J Haematol 1978;39(1):129–46.
[58] Kakudo N, Minakata T, Mitsui T, Kushida S, Notodihardjo FZ, Kusumoto K. Proliferation-promoting effect of platelet-rich plasma on human adipose-derived stem cells and human dermal fibroblasts. Plast Reconstr Surg 2008;122(5):1352–60.
[59] Bir SC, Esaki J, Marui A, Yamahara K, Tsubota H, Ikeda T, et al. Angiogenic properties of sustained release platelet-rich plasma: characterization in-vitro and in the ischemic hind limb of the mouse. J Vasc Surg 2009;50(4):870–9. e872.
[60] Carmeliet P. Angiogenesis in health and disease. Nat Med 2003;9(6):653–60.
[61] Ferrara N. Role of vascular endothelial growth factor in regulation of physiological angiogenesis. Am J Physiol Cell Physiol 2001;280(6):C1358–1366.
[62] De Marchis F, Ribatti D, Giampietri C, Lentini A, Faraone D, Scoccianti M, et al. Platelet-derived growth factor inhibits basic fibroblast growth factor angiogenic properties in vitro and in vivo through its alpha receptor. Blood 2002;99(6):2045–53.
[63] Facchiano A, De Marchis F, Turchetti E, Facchiano F, Guglielmi M, Denaro A, et al. The chemotactic and mitogenic effects of platelet-derived growth factor-BB on rat aorta smooth muscle cells are inhibited by basic fibroblast growth factor. J Cell Sci 2000;113(Pt 16):2855–63.
[64] Muller G, Behrens J, Nussbaumer U, Bohlen P, Birchmeier W. Inhibitory action of transforming growth factor beta on endothelial cells. Proc Natl Acad Sci USA 1987;84(16):5600–4.
[65] Tengood JE, Ridenour R, Brodsky R, Russell AJ, Little SR. Sequential delivery of basic fibroblast growth factor and platelet-derived growth factor for angiogenesis. Tissue Eng Part A 2011;17(9–10):1181–9.
[66] Patel ZS, Young S, Tabata Y, Jansen JA, Wong ME, Mikos AG. Dual delivery of an angiogenic and an osteogenic growth factor for bone regeneration in a critical size defect model. Bone 2008;43(5):931–40.
[67] Peng H, Wright V, Usas A, Gearhart B, Shen HC, Cummins J, et al. Synergistic enhancement of bone formation and healing by stem cell-expressed VEGF and bone morphogenetic protein-4. J Clin Invest 2002;110(6):751–9.
[68] Ratanavaraporn J, Furuya H, Kohara H, Tabata Y. Synergistic effects of the dual release of stromal cell-derived factor-1 and bone morphogenetic protein-2 from hydrogels on bone regeneration. Biomaterials 2011;32(11):2797–811.

THE JOURNAL OF IMMUNOLOGY

Runx3 Is Required for Full Activation of Regulatory T Cells To Prevent Colitis-Associated Tumor Formation

Manabu Sugai, Koji Aoki, Motomi Osato, Yukiko Nambu, Kosei Ito, Makoto M. Taketo and Akira Shimizu

J Immunol 2011;186;6515-6520; Prepublished online 22 April 2011;
doi:10.4049/jimmunol.1001671
http://www.jimmunol.org/content/186/11/6515

The Journal of Immunology is published twice each month by
The American Association of Immunologists, Inc.,
9650 Rockville Pike, Bethesda, MD 20814-3994.

Print ISSN: 0022-1767 Online ISSN: 1550-6606.

Runx3 Is Required for Full Activation of Regulatory T Cells To Prevent Colitis-Associated Tumor Formation

Manabu Sugai,[*,1] Koji Aoki,[†,1] Motomi Osato,[‡,§,¶,‖] Yukiko Nambu,[*,#] Kosei Ito,[**] Makoto M. Taketo,[†] and Akira Shimizu[*]

Inflammation is increasingly recognized as an essential component of tumorigenesis, which is promoted and suppressed by various T cell subsets acting in different ways. It was shown previously in *Runx3*-deficient mice that differentiation of CD8 T and NK cells is perturbed. In this study, we show that *Runx3* is also required for proper differentiation and function of regulatory T cells. In *Runx3*-deficient mice, T cells were unable to inhibit inflammation and to suppress tumor development. As expected, recombination activating gene 2-deficient mice bearing *Runx3*-deficient lymphocytes spontaneously developed colon tumors. However, tumor formation was completely blocked by transfer of either regulatory T cells or CD8 T cells derived from wild-type mice to mutant mice or by housing mutant mice in a specific pathogen-free condition. These results indicate that *Runx3*-deficient lymphocytes and microorganisms act together to induce inflammation and consequently induce the development of colon tumors. *The Journal of Immunology*, 2011, 186: 6515–6520.

Colitis-associated cancer is the most serious complication of inflammatory bowel disease (IBD) (1). Accumulating evidence indicates that immune responses have positive and negative roles in tumor formation (2) and maintenance; chronic inflammatory disease increases the risk of cancer development (3–5), whereas the suppression of immune responses against tumors by enhancing regulatory T cell (Treg) activity allows tumor cells to survive (6). Thus, to maintain a tumor-free status, it is important for the host to respond appropriately during the course of inflammation and tumor formation. TGF-β1 is essential for the maintenance of inflammatory homeostasis, and the loss of the TGF-β1 signaling pathway results in severe inflammation and malignant tumor formation (7), especially in adenomatous polyposis coli (*Apc*) mutant mice (8). T cells are known to be among the targets of the TGF-β1 signaling pathway because T cell-specific deletion of Smad4 results in spontaneous gastrointestinal cancer (9). It has been demonstrated that various CD4 T cell subsets differ in their ability to inhibit or enhance IBD and that these T cell subsets act cooperatively in immune surveillance against tumors. The functional balance of various T cell subsets therefore plays a central role in maintaining the integrity of the epithelial barrier and inhibiting tumor formation in the gastrointestinal tract.

Acting downstream of TGF-β1 signaling, Runx proteins are the interacting and functional partners of R-Smad proteins (10–13). The loss of Runx proteins in lymphocytes can therefore affect the severity of inflammation in the gastrointestinal tract and the incidence of tumor formation. Among the three Runx proteins, Runx3 is involved in the differentiation of immune cells, including CD8 and NK cells (14–17), both of which have cytotoxic activity against tumors. Furthermore, *Runx3*-deficient mice have defects in a subset of dendritic cell (18) and B cell functions (19). Thus, *Runx3*$^{-/-}$ mice are severely compromised immunologically. The functions of Runx3 are not limited to lymphoid tissues, and this protein is also involved in the regulation of epithelial homeostasis, acting within the epithelium of the gastrointestinal tract. Ito and colleagues (20) have demonstrated that *Runx3*$^{-/-}$ gastric epithelial cells are resistant to the growth-inhibitory and apoptosis-inducing action of TGF-β1, resulting in hyperplasia of the gastric mucosa. In addition, Runx3 was shown to attenuate β-catenin/T cell factor functions in intestinal tumorigenesis (21). These data indicate that Runx3 is a tumor suppressor acting in the gastrointestinal epithelium. This notion is strongly supported by the analysis of human tumors. Contrary to these results, Groner and colleagues (22) have demonstrated that *Runx3*$^{-/-}$ mice develop spontaneous IBD and gastric hyperplasia. Because Runx3 was expressed at a high level in lymphoid and myeloid cells, these authors concluded that the colitis and gastric lesions in *Runx3*$^{-/-}$ mice result from the loss of Runx3 in leukocytes (22). However, both groups performed the experiments in mice that were deficient in Runx3 in all tissues, including epithelium and lymphocytes. Therefore, their conclusion needs further investigation. To determine whether hyperplastic changes in the intestines in *Runx3*$^{-/-}$ mice are caused by a defect of epithelial cells or blood cells, Ito et al. (21) generated mice whose leukocytes, but not epithelial cells, were *Runx3*$^{-/-}$ by transplanting bone marrow cells from *Runx3*$^{-/-}$ mice into irradiated wild-type (WT) mice. These mice showed no symptoms of hyperplasia or dysplasia in the intestines 1 y after

*Department of Experimental Therapeutics, Translational Research Center, Kyoto University Hospital, Sakyo-ku, Kyoto 606-8507, Japan; †Department of Pharmacology, Graduate School of Medicine, Kyoto University, Sakyo-ku, Kyoto 606-8501, Japan; ‡Cancer Science Institute of Singapore, National University of Singapore, Singapore 117456; §Institute of Molecular and Cell Biology, Proteos, Singapore 138673; ¶Nanyang Technological University, Singapore 637551; ‖Institute of Bioengineering and Nanotechnology, Singapore 138669; #Department of Clinical Molecular Biology, Kyoto University Hospital, Sakyo-ku, Kyoto 606-8507, Japan; and **Graduate School of Biomedical Sciences, Nagasaki University, Nagasaki 852-8588, Japan

[1]M.S. and K.A. contributed equally to this work.

Received for publication May 19, 2010. Accepted in revised form March 21, 2011.

This work was supported in part by Grants-In-Aid for Science Research on Priority Areas from the Ministry of Education, Culture, Sports, Science and Technology of Japan. Y.N. is a fellow of the Japan Society for the Promotion of Science.

Address correspondence and reprint requests to Dr. Manabu Sugai and Dr. Akira Shimizu, Department of Experimental Therapeutics, Translational Research Center, Kyoto University Hospital, 54 Shogoin-Kawahara-cho, Sakyo-ku, Kyoto 606-8507, Japan. E-mail addresses: msugai@virus.kyoto-u.ac.jp and shimizu@virus.kyoto-u.ac.jp

Abbreviations used in this article: FLC, fetal liver cell; FLT, fetal liver cell transfer; IBD, inflammatory bowel disease; iTreg, inducible regulatory T cell; nTreg, natural regulatory T cell; SPF, specific pathogen-free; Teff, effector T; Treg, regulatory T cell; WT, wild-type.

www.jimmunol.org/cgi/doi/10.4049/jimmunol.1001671

transplantation (21). This observation supports the direct involvement of epithelial cells in tumor formation in *Runx3*$^{-/-}$ mice. However, we cannot rule out the involvement of WT-derived radio-resistant lymphocytes in maintaining the health of intestinal epithelial cells. To exclude this possibility, we used recombination activating gene 2 knockout (*Rag2*$^{-/-}$) mice as recipients because Rag2 is a essential factor for lymphocyte generation.

In this article, we examined whether the loss of functioning Runx3 in lymphocytes contributes to these phenotypes. We found that loss of Runx3 in T cells resulted in suppression of Treg function and that this suppression was the primary cause of colitis but not gastritis observed in *Runx3*$^{-/-}$ mice. In addition, we assessed tumor formation in the colon. All mice bearing *Runx3*$^{-/-}$ lymphocytes, but not WT mice, developed tumors in the large intestine or cecum when they were housed in a conventional mouse facility. However, tumor formation was completely blocked by housing them in a specific pathogen-free (SPF) condition, indicating that microorganisms are involved in this process. Furthermore, no tumor formation was observed when CD8 T cells or Tregs of WT origin were transferred into mutant mice. These results, in addition to previous observations, suggest that Runx3 is a suppressor of gastrointestinal tract tumors acting in lymphocytes and epithelial cells.

Materials and Methods

Mice

WT, *Runx3*$^{+/-}$, and *Rag2*$^{-/-}$mice with the C57BL/6 genetic background were maintained in an SPF mouse facility. For some experiments, mice that received transfers of fetal liver cells (FLCs) were maintained in a conventional mouse facility. Procedures involving animals and their care were conducted according to the guidelines for animal treatment of the Institute of Laboratory Animals, Kyoto University.

Fetal liver transfer

Single-cell suspensions of 2×10^6 to 4×10^6 whole fetal liver mononuclear cells harvested from *Runx3*$^{-/-}$and WT embryos at E14.5 were injected intravenously into sublethally irradiated (4 Gy) male *Rag2*$^{-/-}$ recipient mice. Mice were sacrificed at least 10 wk after transplantation, and cell compartments were analyzed by flow cytometry or used for in vitro culture. All *Rag2*$^{-/-}$mice, which were used for a series of experiments comparing the effects of Runx3, were age-matched, and FLCs from littermates were used.

Histologic analysis

The colon and cecum were removed from mice after euthanasia and dissected free from the anus to a point distal to the cecum and the small intestine. Contents were removed and cleaned with PBS prior to fixation in 4% paraformaldehyde and routine paraffin embedding. Sections were then cut and stained with H&E.

Cell preparation

Naive CD4 T, CD8 T, and Tregs were prepared by magnetic cell sorting using appropriate isolation kits (Miltenyi Biotec, Bergisch Gladbach, Germany). For some experiments, a $CD62L^+CD44^-CD25^-CD4^+$ population was isolated to provide naive CD4 T cells by flow cytometry with a FACSAria (Becton Dickinson, Mountain View, CA).

Cell cultures

In all experiments, the percentages of $CD62L^+CD4^+$ T cells or $CD4^+CD25^+$ T cells were >95%. Naive $CD4^+$ T cells were activated with plate-bound anti-CD3 (5 μg/ml), soluble anti-CD28 (1 μg/ml), anti–IFN-γ (10 μg/ml), and anti–IL-4 (10 μg/ml) in the presence or absence of TGF-β1 (3 ng/ml).

Flow cytometric analysis

The following Abs were used for staining: FITC anti-mouse Foxp3 (eBioscience, San Diego, CA); biotin anti-mouse CD25 (BD Pharmingen, San Diego, CA); allophycocyanin anti-mouse CD4 (BD Pharmingen); PE anti-mouse CD8 (BD Pharmingen); and PerCP–streptavidin (Molecular Probes, Eugene, OR). All analyses were performed with FACSCalibur or FACSAria (Becton Dickinson).

Retroviral infection

Retrovirus was produced by transfecting the ecotropic Plat-E packaging cell line (23) with pMSCV-IRES-hCD4 retroviral vector (24). After stimulation with plate-bound anti-CD3 and soluble anti-CD28 for 24 h, purified naive CD4 T cells were spin-infected with the virus-containing supernatant in the presence of 4 mg/ml polybrene for 1.5 h at 2500 rpm and 32°C and cultured for 48 h.

After removing virus-containing supernatants, cells were reactivated with plate-bound anti-CD3 (5 μg/ml), soluble anti-CD28 (1 μg/ml), anti–IFN-γ (10 μg/ml), and anti–IL-4 (10 μg/ml) in the presence or absence of TGF-β1 (3 ng/ml).

RT-PCR and real-time PCR

Total RNAs were extracted from cultured T cells or sorted cultured T cells using TRIzol (Life Technologies-BRL, Gaithersburg, MD). Oligonucleotide-primed cDNAs were prepared with reverse transcriptase. For semiquantitation, 50 ng cDNA was serially diluted and subjected to PCR amplification. All PCR products were resolved electrophoretically in 2% agarose gel and visualized by ethidium bromide staining. For real-time PCR, RT-PCR was performed using 2× SYBER PCR Master Mix (Qiagen). Specific primer pairs used for real-time PCR were as follows: Runx3 forward (5′-ACCACGAGCCACTTCAGCAG-3′) and Runx3 reverse (5′-CGATGGTGTGGCGCTGTA-3′); Foxp3 forward (5′-GCATGTTCGCCTACTTCAGAAA-3′) and Foxp3 reverse (5′-CCACTCGCACAAAGCACTTG-3′); granzyme B forward (5′-CTCCACGTGCTTTCACCAAA-3′) and granzyme B reverse (5′-AGGATCCATGTTGCTTCTGTAGTTAG-3′); Hprt forward (5′-GTTGGATACAGGCCAGACTTTGTTG-3′) and Hprt reverse (5′-GATTCAACTTGCGCTCATCTTAGGC-3′). Relative expression of mRNA was normalized to Hprt mRNA levels within each sample.

Results

Runx3 *deficiency in lymphocytes leads to the development of spontaneous colitis but not gastritis*

To determine whether Runx3 expression in lymphocytes affects the homeostasis of gastrointestinal epithelial cells, FLCs from

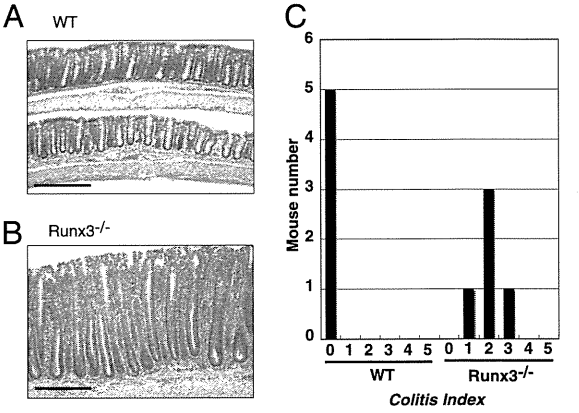

FIGURE 1. Representative photographs of the colon of *Rag2*$^{-/-}$ mice 10 wk after transfer of FLCs from WT and *Runx3*$^{-/-}$ mice. Samples taken from Lymph-*Runx3*$^{-/-}$ or Lymph-WT mice were fixed, sectioned, and stained. Specimens were stained with H&E. Scale bars, 400 μm. *A*, Normal appearance of the colon in a mouse that received WT FLCs. *B*, Moderate colitis in a mouse that received Runx3$^{-/-}$ FLC. *C*, Colitis grades are shown as the colitis index. Colitis was scored from 0 to 5 in a blinded fashion. Histologic features were graded as follows: 0, no inflammation; 1, minimal scattered mucosal inflammatory cell infiltrates, with or without minimal epithelial hyperplasia; 2, mild scattered to diffuse inflammatory cell infiltrates, sometimes extending into the submucosa and associated with erosions, with minimal to mild epithelial hyperplasia and minimal to mild mucin depletion from goblet cells; 3, mild to moderate inflammatory cell infiltrates, often associated with ulceration, with moderate epithelial hyperplasia and mucin depletion; 4, marked inflammatory cell infiltrates, often associated with ulceration, with marked epithelial hyperplasia and mucin depletion; 5, marked transmural inflammation with severe ulceration and loss of intestinal glands. Runx3$^{-/-}$, Lymph-Runx3$^{-/-}$ mice; WT, Lymph-WT mice.

Runx3$^{-/-}$embryos and control littermates were transferred into irradiated *Rag2*$^{-/-}$ mice, and inflammatory status was assessed 10 wk after FLC transplantation ("Lymph-*Runx3*$^{-/-}$" or "Lymph-WT" mice; Runx3$^{-/-}$ and WT indicate the genotypes of transferred FLCs). As shown in Fig. 1*A*, 1*B*, Lymph-*Runx3*$^{-/-}$ mice exhibited spontaneous colitis, but the colitis was not as severe as previously described (22) (Fig. 1*C*). To assess whether the severity of colitis depended on the time course of the disease, we examined the colitis index (25) over a more extended period. The colitis index did not change during the course of our observations from 10 to 65 wk after fetal liver cell transfer (FLT) (Fig. 1*C* and data not shown). These results indicate that Runx3 deficiency in lymphocytes is not sufficient to induce severe colitis, as previously demonstrated (22), at least in this experimental setting. In addition, no Lymph-Runx3$^{-/-}$ mice had gastric hyperplasia. Accordingly, functions of Runx3 in other cell types, but not in lymphocytes, also contribute to the inflammatory status in the gastrointestinal tract.

Runx3 is required for proper Treg function

Because Tregs are important in preventing an excessive inflammatory reaction in the gastrointestinal tract, we examined Foxp3-expressing natural Tregs (nTregs) in the thymus, spleen, and lymph nodes of Lymph-*Runx3*$^{-/-}$ mice. The percentages and numbers of Foxp3$^+$ cells were essentially the same in the different genotypes (Fig. 2*A* and data not shown), indicating that nTreg

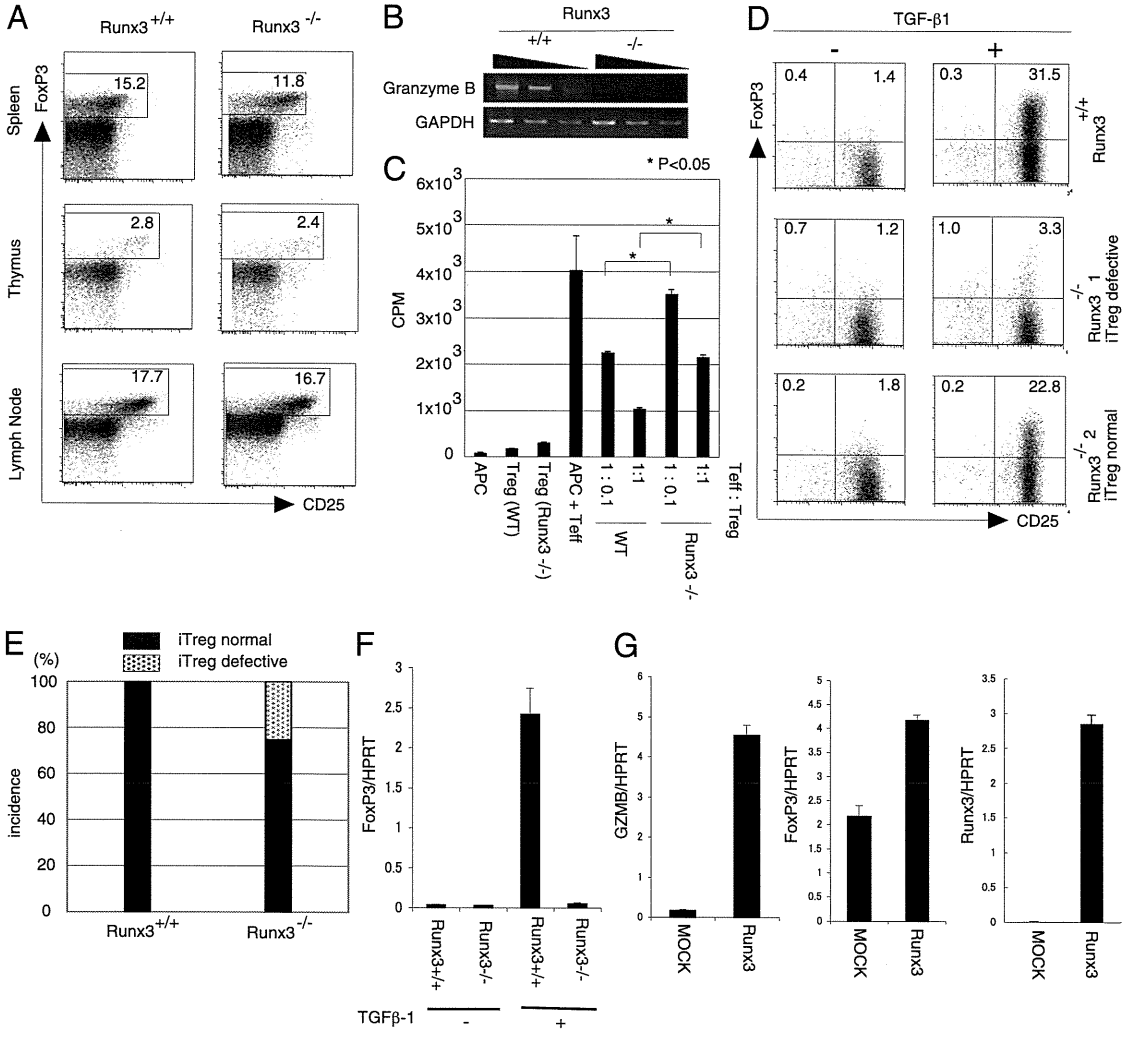

FIGURE 2. Runx3 is required for Treg function. *A*, FACS analysis of spleen cells, thymocytes, and lymph node cells from Lymph-*Runx3*$^{-/-}$ (*Runx3*$^{-/-}$) and Lymph-WT (*Runx3*$^{+/+}$) mice. All plots are gated on CD4$^+$CD8$^-$ cells. Numbers indicate the percentages of Foxp3$^+$ cells. Data are representative of six independent experiments. *B*, CD4$^+$CD25$^+$ cells were cultured with anti-CD3 and IL-2 for 48 h. RNA was prepared, and expression of granzyme B was determined by RT-PCR. GAPDH was used as an internal control for RT-PCR. Data are representative of three independent experiments. Fivefold serial dilutions of cDNAs were amplified for the indicated transcripts. *C*, Suppression assays. CD4$^+$CD25$^-$ responder T cells (2×10^4 cells) were placed in 96-well round-bottom plates with CD4$^+$CD25$^+$ cells and APCs (2×10^4 cells, T cell-depleted spleen cell populations irradiated with 2000 rad) at 37°C in 7% CO_2 and were stimulated for 72 h with mAb to CD3 (1 μg/ml). After 72 h of incubation, cultures were pulsed with [^{3}H]thymidine (1 mCi) 6 h before collection. Teff cells from WT mice were cultured with APC plus anti-CD3 with the indicated ratios of Tregs derived from Lymph-*Runx3*$^{-/-}$ or Lymph-WT mice. The *p* values were calculated by Student *t* test. *$p < 0.05$. *D*, Foxp3 staining of CD4$^+$ T cells after culture with the indicated agents. Numbers shown in the *upper-right corners* indicate the percentages of CD4$^+$Foxp3$^+$ cells. Data are representative of 12 independent experiments. *E*, In each experiment shown in *D*, cells were classified into competent and defective groups with respect to iTreg differentiation. "iTreg normal" (black bar), iTreg competent group in which >20% cells expressed Foxp3; "iTreg defective" (dotted bar), <5% cells expressed Foxp3. *F*, Expression of Foxp3 was determined by real-time PCR using RNA from cultures shown in *D* (*Runx3*$^{+/+}$ and *Runx3*$^{-/-}$-1, iTreg defective). Hprt was used for normalization. *G*, Real-time PCR analysis of granzyme B (GZMB) and Foxp3 expression using cDNAs from retroviral expression of Runx3 in *Runx3*$^{-/-}$ T cells. Hprt was used for normalization. *Runx3*$^{+/+}$, Lymph-WT mice or cells derived from these mice; *Runx3*$^{-/-}$, Lymph-*Runx3*$^{-/-}$ mice or cells derived from these mice.

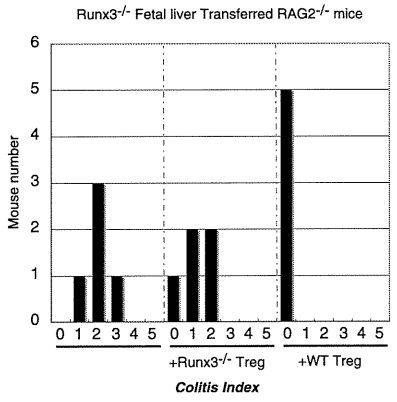

FIGURE 3. Colitis in Lymph-*Runx3*$^{-/-}$ mice is rescued by cotransfer of WT Tregs. Colitis indexes of Lymph-*Runx3*$^{-/-}$ mice were examined 10 wk after transfer of FLT with or without cotransfer of WT or *Runx3*$^{-/-}$ Tregs. Colitis index criteria are described in the legend of Fig. 1.

differentiation in vivo is normal in Lymph-*Runx3*$^{-/-}$ mice. We then examined the expression of essential factors required for Treg function and found that expression of granzyme B (26) was specifically inhibited by the loss of Runx3 (Fig. 2*B*). Because granzyme B and Foxp3 are required for proper nTreg functions, nTregs from Lymph-*Runx3*$^{-/-}$ mice were assessed for suppressive activity in vitro. As shown in Fig. 2*C*, nTregs from Lymph-WT mice

A

FL Genotype	Co-transferred cells	Facility	Tumor	Incidence (%)	
Wild type		SPF	0 / 6	0	
Runx3-/-		SPF	0 / 6	0	
Wild type		Conventional	0 / 6	0	*
Runx3-/-		Conventional	6 / 6	100	*
Runx3-/-	+/+ Regulatory T cells	Conventional	0 / 6	0	*
Runx3-/-	+/+ $CD8^+$ T cells	Conventional	0 / 6	0	*

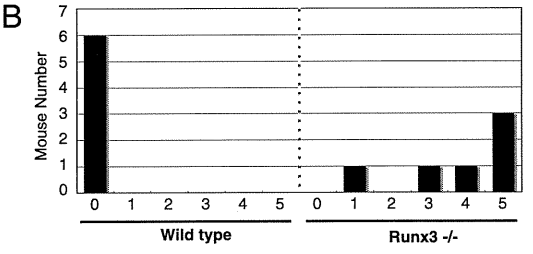

FIGURE 4. Microorganisms increase the severity of colitis and result in tumor formation in Lymph-*Runx3*$^{-/-}$ mice. *A* and *B*, Tumor incidence and the colitis index were examined around 65 wk after FLT transfer. *A*, Tumor incidence. Tumor incidences are shown as X/Y, where X is the number of tumor-bearing mice and Y is the number of mice examined. Significance of differences between groups were estimated by Fisher's exact test with Bonferroni correction. *$p = 0.0022$. *B*, Colitis index after 65 wk of housing in a conventional mouse facility. Colitis index criteria are described in the legend of Fig. 1. The SPF facility was free from the following pathogens: 1, *Citrobacter rodentium*; 2, *Corynebacterium kutscheri*; 3, *Mycoplasma pulmonia*; 4, *Pasteurella pneumotropica*; 5, *Salmonella* spp.; 6, *Pseudomonas aeruginosa*; 7, *Clostridium piliforme*; 8, ectromelia virus; 9, LCM virus; 10, mouse hepatitis virus; 11, Sendai virus; 12, ectoparasites; 13, intestinal protozoa; 14, pinworm; 15, *Pneumocystis carinii*; 16, *Helicobacter hepaticus*; 17, *Helicobacter bilis*. The conventional facility was free from the following pathogens: 1, *Citrobacter rodentium*; 2, *Corynebacterium kutscheri*; 3, *Mycoplasma pulmonia*; 4, *Pasteurella pneumotropica*; 5, *Salmonella* spp.; 6, *Pseudomonas aeruginosa*; 7, *Clostridium piliforme*; 8, mouse hepatitis virus; 9, Sendai virus; 10, intestinal protozoa; 11, dermatophytes; 12, *Staphylococcus aureus*. Co-transferred cells, cells cotransferred with FLCs; FL Genotype, genotypes of the FLCs transferred into *Rag2*$^{-/-}$ mice; *Runx3*$^{-/-}$, Lymph-*Runx3*$^{-/-}$ mice; Wild type, Lymph-WT mice.

at a 1:1 ratio of effector T (Teff) cells to nTregs suppressed the proliferation of Teff cells by >75%, whereas Tregs from Lymph-*Runx3*$^{-/-}$ mice suppressed Teff cell proliferation by <50%. The reduced suppressive activity of nTregs from Lymph-*Runx3*$^{-/-}$ mice was also observed at other nTreg/Teff cell ratios. Thus, nTreg function is perturbed in Lymph-*Runx3*$^{-/-}$ mice. The suppression of nTreg function may be a mechanism that contributes to the colitis observed in Lymph-*Runx3*$^{-/-}$ mice. We next examined the potential role of Runx3 in inducible regulatory T cell (iTreg) generation by adding TGF-β1 in vitro. The involvement of Runx3 in iTreg differentiation is limited, because in 75% of the experiments, *Runx3*$^{-/-}$ naive CD4 T cells differentiated to iTregs, which is similar to the result obtained for WT cells (*upper* and *lower rows* of Fig. 2*D*, 2*E*). However, in only 25% of the experiments were *Runx3*$^{-/-}$ T cells defective in differentiation to iTregs, as shown in Fig. 2*D* (*middle row*) and Fig. 2*E*. In this case, fewer $Foxp3^+$ cells caused transcriptional inhibition of the Foxp3 gene in *Runx3*-deficient T cells (Fig. 2*F*). The function of Runx3 in Foxp3 transcription was further confirmed by forced expression of Runx3 in *Runx3*$^{-/-}$ CD4 T cells (27–30). Thus, Runx3 proteins stimulate the expression of Foxp3 and granzyme B (Fig. 2*G*). At this time, it is unclear why iTreg differentiation fluctuated in different samples of *Runx3*-deficient cells (*middle* and *lower columns* in Fig. 2*D*, 2*E*). Further experiments will be required to elucidate this important issue.

To determine further the involvement of Tregs in the observed colitis in Lymph-*Runx3*$^{-/-}$ mice, we transferred nTregs together with *Runx3*$^{-/-}$ FLCs into irradiated *Rag2*$^{-/-}$ mice. As shown in Fig. 3, the severity of colitis was assessed 10 wk after FLT transfer. nTregs from Lymph-WT mice completely inhibited colitis; the colitis index was 0 in all mice. In contrast, slight improvements in the colitis index were observed when nTregs from Lymph-*Runx3*$^{-/-}$ mice were used. Taking these results together with the in vitro data, *Runx3*$^{-/-}$ nTregs appear to be

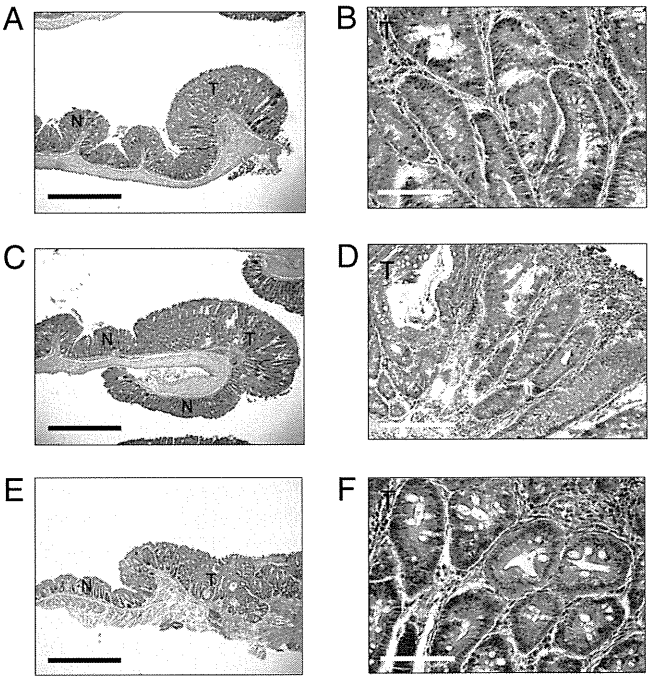

FIGURE 5. Representative tumors of Lymph-Runx3$^{-/-}$ mice in large intestine (*A–D*) and cecum (*E*, *F*). Enlarged pictures of tumor regions are shown at right (*B*, *D*, *F*). Specimens were stained with H&E. Black scale bars, 1 mm (*A*, *C*, *E*); white scale bars, 100 μm (*B*, *D*, *F*). N, normal regions; T, tumors.

functionally defective, which may be a cause of colitis induced in Lymph-*Runx3*$^{-/-}$ mice.

Runx3-*deficient CD8 T cells, Tregs, and microorganisms are required for the development of colitis-associated tumors in lymph*-Runx3$^{-/-}$ *mice*

Our previous experiments (20, 21) indicated that loss of Runx3 in epithelial cells of the gastrointestinal tract causes hyperplasia of the gastric mucosa and the formation of intestinal tumors. In those experiments, we excluded the possibility of the involvement of lymphocytes in colitis and tumor formation by transplanting bone marrow cells from *Runx3*$^{-/-}$ mice into irradiated WT mice (21). However, this procedure is not suitable for assessing the functions of Tregs because ~5% of the lymphocytes survive after irradiation, and the remaining Tregs affect the result. To examine further the possible role of Tregs in colitis, we transferred *Runx3*$^{-/-}$ FLCs into *Rag2*$^{-/-}$ mice, which have no lymphocytes because of a defect in VDJ recombination. As demonstrated earlier, *Runx3*-deficient Tregs are one of the causes of colitis in *Runx3*$^{-/-}$ mice. In our previous report (21), we also demonstrated that small intestinal adenomas developed in *Runx3*$^{+/-}$ mice at around 65 wk of age, with an incidence rate of 54%. We therefore examined the involvement of *Runx3*$^{-/-}$ lymphocytes in intestinal tumor formation using Lymph-*Runx3*$^{-/-}$ mice. Unexpectedly, no tumor formation was observed in these mice. Because the colonic lumen contains abundant commensal bacteria and the composition of this population plays an essential role in colitogenesis, the same assays were performed after housing Lymph-*Runx3*$^{-/-}$ mice in a conventional mouse facility. In this case, all Lymph-*Runx3*$^{-/-}$ mice developed tumors in the large intestine or cecum (Fig. 4*A*; 100% in Lymph-*Runx3*$^{-/-}$ mice compared with 0% in Lymph-WT mice). The colitis index was also increased in Lymph-*Runx3*$^{-/-}$ mice but not in Lymph-WT mice (Fig. 4*B*). A representative tumor in Lymph-*Runx3*$^{-/-}$ mice is shown in Fig. 5. Notably, it contained abundant stromal cells, such as lymphocytes, fibroblasts, macrophages, and smooth muscle fibers, whereas changes in the epithelial cells were milder and different from typical adenomas observed in *Runx3*$^{+/-}$ mice (Fig. 5). These data suggest that loss of Runx3 activity in lymphocytes contributes to the development of IBD and subsequent colon tumorigenesis. However, the mechanisms of tumorigenesis appear different between Lymph-*Runx3*$^{-/-}$ and *Runx3*$^{+/-}$ mice. To examine further the involvement of CD8 T cells and Tregs in the development of intestinal tumors, CD8 T cells or Tregs of WT origin were cotransferred with *Runx3*$^{-/-}$ FLCs. As shown in Fig. 4*A*, tumors were not formed in the colon in either case. These data indicate that loss of Runx3 in Tregs and CD8 T cells also contributes to tumorigenesis, in addition to colitogenic microorganisms in the colon.

Discussion

Our results show that inactivation of Runx3 in lymphocytes can induce colitis and consequently tumorigenesis in the large intestine. Thus, the inflammatory phenotype observed in Lympho-*Runx3*$^{-/-}$ mice is limited to the large intestine and cecum. However, Groner and colleagues (22) demonstrated that *Runx3*$^{-/-}$ mice developed spontaneous IBD and gastric hyperplasia. This difference suggests several possibilities. In comparison with *Runx3*$^{-/-}$ mice (22), Lymph-*Runx3*$^{-/-}$ mice show a weaker inflammatory phenotype. Thus, it is conceivable that other defects, but not lymphocyte defects, caused by the loss of Runx3 contribute to the severity of inflammation. If the gastric mucosa is more resistant to irritating stimuli than the intestinal mucosa, differences in the phenotype can be explained by this difference in inflammatory severity between these mice. Another possibility is that the gastric epithelium requires more Runx3 activity than the intestinal epithelium to maintain epithelial homeostasis; thus, Lymph-*Runx3*$^{-/-}$ mice do not show gastric hyperplasia because Runx3 expression is not perturbed within the gastric epithelium in Lymph-*Runx3*$^{-/-}$ mice. In addition, differences in the targeting strategy will affect the severity of gastrointestinal inflammation, which will change the expression levels of splicing variants of the Runx3 gene (22). The exact mechanisms of these processes are yet to be clarified.

Runx factors may be involved in Treg functions (29–31). Runx1 makes a greater contribution to Treg function than the two other Runx family proteins because Treg-specific deletion of Runx1 results in gastritis (30). Akdis and colleagues (29) found that Runx1 and Runx3 have some functional redundancy in Tregs in the human. In this report, we have shown that *Runx3*-deficient Tregs have a defect in Treg function in vivo and in vitro. In addition, we have found that colitis worsens when Lymph-*Runx3*$^{-/-}$ mice, but not Lymph-WT mice, are housed in a conventional mouse facility. This indicates that commensal microorganisms and Tregs work together to establish a mutual relationship. Taking these observations into account, we propose that both Runx1 and Runx3 are required for the proper functioning of Tregs in becoming tolerant to intestinal bacteria and establishing a good commensal relationship with various bacterial species. However, how to regulate the balance between inhibiting infection and preventing an excessive inflammatory reaction remains to be clarified. In addition, it is unclear why iTreg differentiation fluctuated in different samples of *Runx3*-deficient cells (Fig. 2*D*, *middle* and *lower columns*, 2*E*). It is likely that fluctuations in compensatory expression or activity of other members of the Runx family in *Runx3*$^{-/-}$ T cells affect the capacity of these cells to differentiate into iTregs. This possibility requires investigation in future studies.

Previous reports indicated that Runx3 is required for the proper differentiation and function of CD8 T cells. We therefore examined the involvement of CD8 T cells in tumor formation and found that these cells prevented colitis-associated tumor formation in our experimental setting. In addition to the essential role of CD8 T cells in tumor immunity, recent data indicate that several subsets of CD8 T cells have the capacity to inhibit immune reactions. In this regard, we have not found any obvious anti-inflammatory effect of CD8 T cells. To reveal the exact functions of CD8 T cells in preventing tumor formation in Lymph-*Runx3*$^{-/-}$ mice remains an important issue for investigation.

Acknowledgments

We thank K. Nakano for technical assistance, K. Ikuta (Institute for Virus Research, Kyoto University) for discussion, T. Kitamura (Institute of Medical Science, University of Tokyo) for Plat-E packaging cells, S. Teramukai (Translational Research Center, Kyoto University) for advice on statistical analysis, and F. Alt (Department of Genetics, Harvard Medical School) for *Rag2*$^{-/-}$ mice.

Disclosures

The authors have no financial conflicts of interest.

References

1. Waldner, M. J., and M. F. Neurath. 2009. Colitis-associated cancer: the role of T cells in tumor development. *Semin. Immunopathol.* 31: 249–256.
2. Sakaguchi, S., T. Yamaguchi, T. Nomura, and M. Ono. 2008. Regulatory T cells and immune tolerance. *Cell* 133: 775–787.
3. Balkwill, F., and A. Mantovani. 2001. Inflammation and cancer: back to Virchow? *Lancet* 357: 539–545.
4. Karin, M., T. Lawrence, and V. Nizet. 2006. Innate immunity gone awry: linking microbial infections to chronic inflammation and cancer. *Cell* 124: 823–835.

5. Garrett, W. S., G. M. Lord, S. Punit, G. Lugo-Villarino, S. K. Mazmanian, S. Ito, J. N. Glickman, and L. H. Glimcher. 2007. Communicable ulcerative colitis induced by T-bet deficiency in the innate immune system. *Cell* 131: 33–45.
6. Kosmaczewska, A., L. Ciszak, S. Potoczek, and I. Frydecka. 2008. The significance of Treg cells in defective tumor immunity. *Arch. Immunol. Ther. Exp. (Warsz.)* 56: 181–191.
7. Markowitz, S., J. Wang, L. Myeroff, R. Parsons, L. Sun, J. Lutterbaugh, R. S. Fan, E. Zborowska, K. W. Kinzler, B. Vogelstein, et al. 1995. Inactivation of the type II TGF-beta receptor in colon cancer cells with microsatellite instability. *Science* 268: 1336–1338.
8. Takaku, K., M. Oshima, H. Miyoshi, M. Matsui, M. F. Seldin, and M. M. Taketo. 1998. Intestinal tumorigenesis in compound mutant mice of both Dpc4 (Smad4) and Apc genes. *Cell* 92: 645–656.
9. Kim, B. G., C. Li, W. Qiao, M. Mamura, B. Kasprzak, M. Anver, L. Wolfraim, S. Hong, E. Mushinski, M. Potter, et al. 2006. Smad4 signalling in T cells is required for suppression of gastrointestinal cancer. *Nature* 441: 1015–1019.
10. Shi, M. J., and J. Stavnezer. 1998. CBF alpha3 (AML2) is induced by TGF-beta1 to bind and activate the mouse germline Ig alpha promoter. *J. Immunol.* 161: 6751–6760.
11. Zhang, Y., and R. Derynck. 2000. Transcriptional regulation of the transforming growth factor-beta -inducible mouse germ line Ig alpha constant region gene by functional cooperation of Smad, CREB, and AML family members. *J. Biol. Chem.* 275: 16979–16985.
12. Pardali, E., X. Q. Xie, P. Tsapogas, S. Itoh, K. Arvanitidis, C. H. Heldin, P. ten Dijke, T. Grundström, and P. Sideras. 2000. Smad and AML proteins synergistically confer transforming growth factor beta1 responsiveness to human germline IgA genes. *J. Biol. Chem.* 275: 3552–3560.
13. Hanai, J., L. F. Chen, T. Kanno, N. Ohtani-Fujita, W. Y. Kim, W. H. Guo, T. Imamura, Y. Ishidou, M. Fukuchi, M. J. Shi, et al. 1999. Interaction and functional cooperation of PEBP2/CBF with Smads. Synergistic induction of the immunoglobulin germline Calpha promoter. *J. Biol. Chem.* 274: 31577–31582.
14. Taniuchi, I., M. Osato, T. Egawa, M. J. Sunshine, S. C. Bae, T. Komori, Y. Ito, and D. R. Littman. 2002. Differential requirements for Runx proteins in CD4 repression and epigenetic silencing during T lymphocyte development. *Cell* 111: 621–633.
15. Sato, T., S. Ohno, T. Hayashi, C. Sato, K. Kohu, M. Satake, and S. Habu. 2005. Dual functions of Runx proteins for reactivating CD8 and silencing CD4 at the commitment process into CD8 thymocytes. *Immunity* 22: 317–328.
16. Ohno, S., T. Sato, K. Kohu, K. Takeda, K. Okumura, M. Satake, and S. Habu. 2008. Runx proteins are involved in regulation of CD122, Ly49 family and IFN-gamma expression during NK cell differentiation. *Int. Immunol.* 20: 71–79.
17. Kohu, K., T. Sato, S. Ohno, K. Hayashi, R. Uchino, N. Abe, M. Nakazato, N. Yoshida, T. Kikuchi, Y. Iwakura, et al. 2005. Overexpression of the Runx3 transcription factor increases the proportion of mature thymocytes of the CD8 single-positive lineage. *J. Immunol.* 174: 2627–2636.
18. Fainaru, O., E. Woolf, J. Lotem, M. Yarmus, O. Brenner, D. Goldenberg, V. Negreanu, Y. Bernstein, D. Levanon, S. Jung, and Y. Groner. 2004. Runx3 regulates mouse TGF-beta-mediated dendritic cell function and its absence results in airway inflammation. *EMBO J.* 23: 969–979.
19. Watanabe, K., M. Sugai, Y. Nambu, M. Osato, T. Hayashi, M. Kawaguchi, T. Komori, Y. Ito, and A. Shimizu. 2010. Requirement for Runx proteins in IgA class switching acting downstream of TGF-beta 1 and retinoic acid signaling. *J. Immunol.* 184: 2785–2792.
20. Li, Q. L., K. Ito, C. Sakakura, H. Fukamachi, K. Inoue, X. Z. Chi, K. Y. Lee, S. Nomura, C. W. Lee, S. B. Han, et al. 2002. Causal relationship between the loss of RUNX3 expression and gastric cancer. *Cell* 109: 113–124.
21. Ito, K., A. C. Lim, M. Salto-Tellez, L. Motoda, M. Osato, L. S. Chuang, C. W. Lee, D. C. Voon, J. K. Koo, H. Wang, et al. 2008. RUNX3 attenuates beta-catenin/T cell factors in intestinal tumorigenesis. *Cancer Cell* 14: 226–237.
22. Brenner, O., D. Levanon, V. Negreanu, O. Golubkov, O. Fainaru, E. Woolf, and Y. Groner. 2004. Loss of Runx3 function in leukocytes is associated with spontaneously developed colitis and gastric mucosal hyperplasia. *Proc. Natl. Acad. Sci. USA* 101: 16016–16021.
23. Morita, S., T. Kojima, and T. Kitamura. 2000. Plat-E: an efficient and stable system for transient packaging of retroviruses. *Gene Ther.* 7: 1063–1066.
24. Gonda, H., M. Sugai, Y. Nambu, T. Katakai, Y. Agata, K. J. Mori, Y. Yokota, and A. Shimizu. 2003. The balance between Pax5 and Id2 activities is the key to AID gene expression. *J. Exp. Med.* 198: 1427–1437.
25. Asseman, C., S. Mauze, M. W. Leach, R. L. Coffman, and F. Powrie. 1999. An essential role for interleukin 10 in the function of regulatory T cells that inhibit intestinal inflammation. *J. Exp. Med.* 190: 995–1004.
26. Gondek, D. C., L. F. Lu, S. A. Quezada, S. Sakaguchi, and R. J. Noelle. 2005. Cutting edge: contact-mediated suppression by CD4+CD25+ regulatory cells involves a granzyme B-dependent, perforin-independent mechanism. *J. Immunol.* 174: 1783–1786.
27. Bruno, L., L. Mazzarella, M. Hoogenkamp, A. Hertweck, B. S. Cobb, S. Sauer, S. Hadjur, M. Leleu, Y. Naoe, J. C. Telfer, et al. 2009. Runx proteins regulate Foxp3 expression. *J. Exp. Med.* 206: 2329–2337.
28. Rudra, D., T. Egawa, M. M. Chong, P. Treuting, D. R. Littman, and A. Y. Rudensky. 2009. Runx-CBFbeta complexes control expression of the transcription factor Foxp3 in regulatory T cells. *Nat. Immunol.* 10: 1170–1177.
29. Klunker, S., M. M. Chong, P. Y. Mantel, O. Palomares, C. Bassin, M. Ziegler, B. Rückert, F. Meiler, M. Akdis, D. R. Littman, and C. A. Akdis. 2009. Transcription factors RUNX1 and RUNX3 in the induction and suppressive function of Foxp3+ inducible regulatory T cells. *J. Exp. Med.* 206: 2701–2715.
30. Kitoh, A., M. Ono, Y. Naoe, N. Ohkura, T. Yamaguchi, H. Yaguchi, I. Kitabayashi, T. Tsukada, T. Nomura, Y. Miyachi, et al. 2009. Indispensable role of the Runx1-Cbfbeta transcription complex for in vivo-suppressive function of FoxP3+ regulatory T cells. *Immunity* 31: 609–620.
31. Ono, M., H. Yaguchi, N. Ohkura, I. Kitabayashi, Y. Nagamura, T. Nomura, Y. Miyachi, T. Tsukada, and S. Sakaguchi. 2007. Foxp3 controls regulatory T-cell function by interacting with AML1/Runx1. *Nature* 446: 685–689.